Morphodynamic network simulations of the Westerschelde

R.J. Fokkink

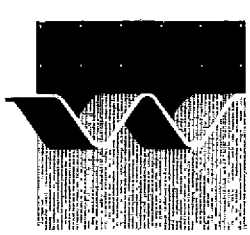

delft hydraulics

delft hydraulics

CLIENT :Directoraat-Generaal Rijkswaterstaat, directie Zeeland

TITLE :Morphodynamic network simulations of the Westerschelde

ABSTRACT : The study describes a morphological model of the Westerschelde . It is a one-dimensional netwrok model, which simulates the water flow and the sediment transports. The model is calibrated with special attention to the asymmetries of the tidal flow. The morphological devlopment is simulated for the period 1968-78.

REFERENCES:

REV.	ORIGINATOR	DATE	REMARKS	REVIEWED BY	APPROVED BY
	dr. R.J. Fokkink	9 dec 1997		dr. ir. M.J.F. Stive	ir. T.Schilperoort

KEYWORD(S)	CONTENTS	STATUS
	TEXT PAGES : 23 TABLES : 11 FIGURES 19 APPENDICES :	☐ PRELIMINARY ☐ DRAFT ☒ FINAL
	PROJECT IDENTIFICATION:Z919	

Contents

1 Introduction

The Directorate General Rijkswaterstaat/Directie Zeeland and the Rijksinstuut voor Kust en Zee of the Ministry of Public Works and Transport are interested in morphological predictions of the consequences of (human) interference (e.g. dredging, land reclamation) on the geometry of estuaries and tidal basins. Two types of one-dimensional models are being considered:

- A one-dimensional long-term model to predict the morphological development in estuaries and tidal basins over a period of 50 to 100 years (ESTMORF).
- A medium-term model to predict the morphological development in estuaries and tidal basins over a period of 20 to 30 years (EENDMORF). This model is the subject of the present study.

The influence of the boundary condition on the morphological development is studied in a parallel study of Delft University (De Jong and Heemink, 1996).

The long-term model ESTMORF is studied in the DYNASTAR project. The model equations were defined after a literature survey (Karssen and Wang, 1992) in which it was decided to combine concepts of Allersma, Eysink and Di Silvio. The model has been calibrated for the Westerschelde and the Friesche Zeegat. It is currently used to study the impact of gas-mining on the morphology of the Friesche Zeegat. In the near future, the calibration of the Westerschelde model will be improved. The development of the ESTMORF model is funded by RIKZ.

The medium-term model EENDMORF is studied in the OOSTWEST project. The EENDMORF model is morphodynamic and is based on equations for hydrodynamics and sediment transport that are state of the art. This model is the subject of the present study. In previous phases the studies were theoretical, concentrating on the sediment distribution over bifurcating channels. Subsequently, the theoretical findings were tested in simple network models and in a one channel model of the Westerschelde. The present study concerns the implementation of a morphodynamic network model in the one-dimensional package SOBEK.

1.1 Contents of this study

The present study aims to put the EENDMORF model to a practical use. Previously, the EENDMORF study has been theoretical and focused on the behaviour of simple pilot models. In the ESTMORF study a dynamic/empirical model of the Westerschelde has already been developed 3 years ago (Karssen, 1994). Even though the calibration of ESTMORF has not been completed yet, the present results of that model show a good behaviour for a major part of the estuary (Fokkink, 1997).

The present study contains the following parts:

1. *Simulations of the water flow.*
   In EENDMORF the sediment transports are determined by the hydrodynamic conditions. Thus the calibration on the water flow is of main importance. The flow has been calibrated already in the IMPLIC model, but the morphodynamic model requires a calibration in which the higher harmonics receive more consideration.
2. *Simulations of the sediment transport.*
   Special attention is given to the circulation of the (residual) sediment transport. Furthermore, the influence of the boundary condition is considered.
3. *Simulations of the morphological development.*
   The morphological development is simulated over a period of 10 years, including the effect of the human interference.

Up to now, an operational morphodynamic model on the scale of the Westerschelde has not been reported in the literature. The Westerschelde model was the first implementation in SOBEK of a large scale model for estuarine morphology. It has led to many improvements of SOBEK concerning the computation of the water flow and the sediment transport in an estuary.

2 The water flow

The EENDMORF model is based on the bathymetry of the Westerschelde in 1968. The same bathymetry is also used for the ESTMORF study. It is a bathymetry of the hydrodynamical model IMPLIC. See Figure 2.1 for a layout of the network. The water flow in the model has already been calibrated for the IMPLIC model. However, in EENDMORF this calibration is adjusted, because a morphodynamic model has other priorities than a hydrodynamical model. In a hydrodynamic model it is important to get the global flow velocity and the water level right. In a morphodynamic model it is important to get the residual sediment transports right.

Van der Kreeke and Robaczewska (1995) have shown that the harmonic components M_0, M_2 and M_4 should be calibrated equally well in a morphodynamic model. There is essentially only one parameter to calibrate these three harmonics: the resistance of the bed. The friction parameter depends on place and on the direction of the flow. It is varied in three steps.

1. The average friction is used to calibrate M_2. The resistance does not depend on the flow direction.
2. The flow friction is varied with the direction of the flow to calibrate M_4. The parameter is varied for large regions of the estuary, keeping the average resistance as found in (1) invariant.
3. The flow dependent friction is varied locally for ebb channels and flood channels to calibrate M_0.

The results of SOBEK are compared to those of IMPLIC to see if there are any major differences between these models, in section 2.1. The calibration of the flow is discussed in section 2.2 - 2.7.

2.1 A comparison of IMPLIC and SOBEK

The IMPLIC bathymetry has to be translated to a SOBEK bathymetry, because the models define cross sections in a slightly different way. IMPLIC uses *flow area*, *storage width* and *hydraulic radius* at levels with fixed intervals of 0.5 m, starting from -2.5 m (NAP). SOBEK uses *flow width* and *storage width* at varying intervals. So the flow area in IMPLIC has to be replaced by flow width in SOBEK. The hydraulic radius which is an extra parameter in IMPLIC, is computed internally by SOBEK. If $A(n)$ denotes the flow area below the level of $0.5n$-2.5 m (NAP), then $(A(n)-A(n-1))/0.5$ is the flow width at this level in SOBEK.

The bathymetry of the Western Scheldt contains structures (weirs). In the morphological simulations, these structures caused numerical instabilities. Therefore, the structures are removed in the SOBEK model. Now the following comparisons are made:

1. The SOBEK model and the IMPLIC model without structures, see Figure 2.2
2. The SOBEK model and the IMPLIC model with structures, see Figure 2.3

Figure 2.2 shows that there is a small difference between IMPLIC and SOBEK, in particular for the initial time steps. This is because SOBEK and IMPLIC use a different initial condition. As the influence of the initial condition decreases, so does the difference between SOBEK and IMPLIC. When the flow is fully adapted to the boundary conditions, the difference is in the order of a few cm. This may be explained by the fact that IMPLIC uses the hydraulic radius as an extra input parameter while SOBEK does not.

Figure 2.3 shows that removing the structures effects the water flow, in particular for the high water levels in the eastern part of the estuary. Most of the structures are located between Bath and Antwerp. Still, the difference between SOBEK without structures and IMPLIC with structures is relatively small up to Bath.

2.2 The harmonic components of the tide

The calibration of the flow focuses on the harmonics M_0, M_2 and M_4. Therefore, the water flow is calibrated for an M_2M_4 tide at the open sea boundary, so there is no interference of other components. The M_2M_4 tide and the average tide at Vlissingen are given in Figure 2.4.

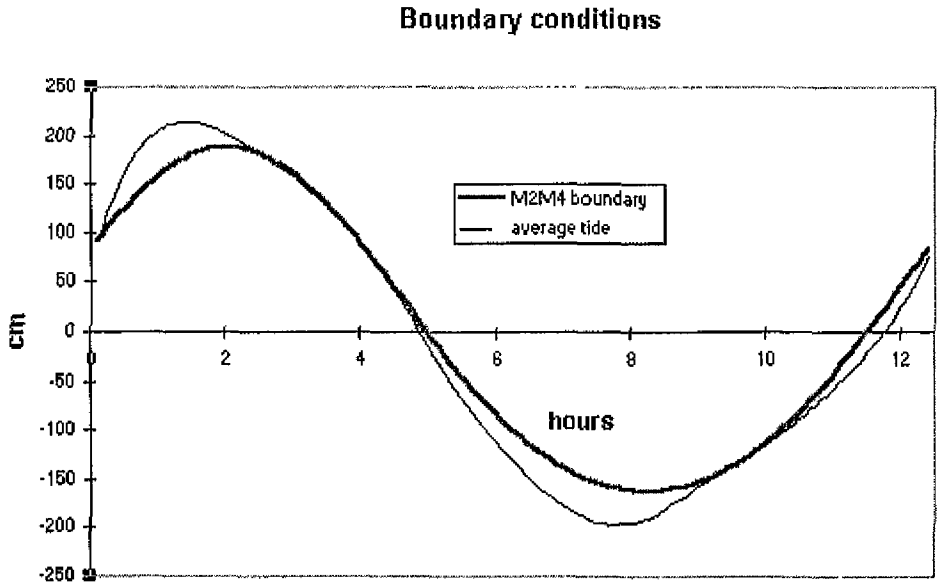

Figure 2.4 The M_2M_4 tide compared to the average tide (different boundary conditions)

The figure shows that there is a considerable difference between the average tide and the M_2M_4 tide. The average tide has a larger amplitude and a greater asymmetry, although this asymmetry may not increase the transport. The residual transports generated by the average tide may therefore be larger than the transports generated by the M_2M_4 tide. Therefore, in the simulations of the sediment transport and the morphological development (Chapter 3 and 4) both boundary conditions are considered.

The tidal range for the average tide is 4.2 m compared to 3.5 m for the M_2M_4 tide.

2.3 The relative error of the calibration

The aim of the model is to simulate the sediment transport in the Westerschelde. The water flow should therefore be calibrated in such a way that the (residual) sediment transport is represented as well as possible. The relative error of the (residual) sediment transport should be minimised.

Van der Kreeke and Robaczewska (1995) have shown how the water flow should be calibrated in a morphodynamic model. Their argument is given below. The sediment transport S is given by a power law of the flow velocity u

$$S = Mu^5 \tag{2-1}$$

The transport coefficient M follows from various parameters of the bathymetry and the sediment. The flow velocity u is given by

$$u = u_0 + u_2 \cos\omega t + u_4 \cos(2\omega t + \phi) \tag{2-2}$$

ω = angular frequency of M_2
ϕ = phase lag between M_2 and M_4
u_i = components of the velocity, representing M0, M2 and M4.

An integration over a tidal period gives the residual transport, which is proportional to:

$$\frac{5}{4}u_2^4 u_4 \cos\phi + \frac{15}{8}u_2^4 u_0 \tag{2-3}$$

If the relative errors are denoted by Δ, the relative error in the sediment transport S is given by

$$\Delta S = \left[\frac{15}{2}\Delta u_2 + \frac{5}{4}\Delta u_4 + \frac{5}{4}\Delta\phi + \frac{15}{8}\Delta u_0\right] \tag{2-4}$$

The calibration of the water flow should minimise this term.

2.4 The calibration of M_2

Step 1 of the calibration: M_2 is calibrated by friction, independent of the direction of the flow.

The calibration on M_2 and M_4 is based on the harmonics of the water levels instead of the harmonics of the flow velocity. This is based on the assumption that the amplitude of the water level is proportional to the amplitude of the velocity. This assumption is motivated by the linear relation between tidal amplitude and velocity as observed in nature.

The actual M_2 tidal component is compared to M_2 in the IMPLIC model. It is also compared to the M_2 in the hydrodynamic model for a non-flow dependent bed resistance. The tide at Vlissingen is a boundary condition.

Table 2.1

STATION	ACTUAL M_2	IMPLIC M_2
Vlissingen	1.75m, 59°	1.75m, 59°
Terneuzen	1.87m, 68°	1.89m, 68°
Bath	2.10m, 94°	2.06m, 97°
Antwerp	1.96m, 116°	2.18m, 120°

The table shows that for the M_2-M_4 boundary condition, the amplitude of the model M_2 is too large at Antwerp. Furthermore, averaging the resistance does influence the propagation of M_2.

The M_2 component is calibrated for a friction parameter which does not depend on the direction of the flow. The Westerschelde is divided into four regions: Vlissingen-Terneuzen, Terneuzen-Hansweert, Hansweert-Bath, Bath-Antwerp. In each of these regions, the Manning coefficient is varied as shown in Table 2.2. The table should be read as follows: for run 1, the reciprocal Manning coefficient $1/m$ is unchanged for each model branch in the region Vlissingen-Terneuzen and it is increased by 1 in the region Terneuzen-Hansweert.

Table 2.2: Changes of the reciprocal Manning coefficient

$1/m$	V-T	T-H	H-B	B-A
run 0	0	0	0	0
run 1	0	+1	+1	-1
run 2	-1	+3	+3	-10
run 3	-2	+5	+5	-15
run 4	-2	+7	-3	-10

The results of the amplitude and the phase angle of M_2 are given for these runs in Table 2.3. The main deviation between the model and the data occur at the tidal station Antwerp. Note that the amplitude at Antwerp is too large for the parameter choice of the original IMPLIC model (run 0). A reason for this may be the fact that the IMPLIC model has been calibrated for a different boundary condition.

Table 2.3 Simulated M_2

M_2	Vlis	Tern	Bath	Antw
real	1.75 m 59°	1.87 m 68°	2.10 m 94°	1.96 m 116°
run 0	1.75m, 59°	1.87m, 70°	1.97m, 100°	2.07m, 122°
run 1	1.75 m 59°	1.88 m 70°	2.07 m 97°	2.12 m 121°
run 2	1.75 m 59°	1.88 m 70°	2.09 m 95°	2.04 m 122°
run 3	**1.75 m** **59°**	**1.88 m** **71°**	**2.11 m** **94°**	**1.93 m** **116°**
run 4	1.75 59°	1.88 m 71°	2.07 m 96°	1.96 m 120°

Run 3 gives the best approximation of the M_2 tide for the tidal stations. Note that this runs gives results which are almost identical to the results of run 0 (the original IMPLIC run) for the tidal stations Terneuzen and Bath.

2.5 The calibration of M_4

Step 2 of the calibration. M_4 is calibrated by making friction dependent of the direction of the water flow, keeping the average friction fixed. Here, the flow dependence is varied on a large scale for four regions of the Westerschelde.

After the calibration of M_2 it is necessary to calibrate M_4, keeping M_2 fixed. This is done by introducing a flow-dependent resistance, keeping the average resistance fixed. A physical explanation for this phenomenon is that the density gradient due to salinity causes a flow dependent fiction. Another cause for flow dependant friction is the funnel shape of the estuary.

The actual M_4 tide is compared to the simulated M_4 tide in Table 2.4

Table 2.4 propagation of M_4

M_4	Vlis	Tern	Bath	Antw
real	0.13m 117°	0.12m, 133°	0.12m 167°	0.13m 179°
run 3	0.13m 117°	0.11m, 149°	0.14m 169°	0.20m 189°

The Manning coefficient *m* for the calibration of M_2 did not depend on the direction of the flow. In the calibration of M_4 *m* is varied for the direction of the flow in such a way that the average resistance remains the same. Again the variation is carried out for the four large regions Vlissingen-Terneuzen-Hansweert-Bath. For each channel, the inverse coefficient

$1/m$ is changed by $+\Delta$ in the flood direction and $-\Delta$ in the ebb direction, as shown in Table 2.5. Ebb direction here means the direction of the flow during falling tide.

Table 2.5 change of the reciprocal Manning coefficient $1/m$

Δ	V-T	T-H	H-B	B-A
run 5	+1	+1	-1	-1
run 6	+2	+2	-3	-3
run 7	+4	+4	-6	+2
run 8	+3	+3	-6	+2
run 9	+3	+2	-4	+2
run 10	+3	+2	0	+2
run 11	+3	+2	-8	+2

The resulting propagation of M_4 is given in Table 2.6

Table 2.6 M_4 component

	Vlis	Tern	Bath	Antw
actual	0.13m 117°	0.12m 133°	0.13m 167°	0.13m 179°
run 5	0.13m 117°	0.11m 145°	0.15m 163°	0.21m 184°
run 6	0.13m 117°	0.11m 141°	0.15m 160°	0.19m 197°
run 7	0.13m 117°	0.11m 130°	0.14m 155°	0.16m 199°
run 8	0.13m 117°	0.11m 132°	0.14m 158°	0.15m 200°
run 9	0.13m 117°	0.11m 133°	0.13m 158°	0.17m 191°
run 10	0.13m 117°	0.11m 142°	0.15m 156°	0.24m 168°
run 11	**0.13m 117°**	**0.12m 128°**	**0.15m 165°**	**0.11m 232°**

Run 11 gives the best results and is used for the last step: the calibration of the circulation.

2.6 The calibration of M_0

Step 3 of the calibration. M_0 is calibrated by flow dependent friction, which is varied for individual channels.

The calibration on M_0 is based on residual flows as computed by the 2D DETWES model (Van der Male, 1992). The calibration on M_2-M_4 distinguished four regions of the Westerschelde in which m was varied without consideration of ebb channels and flood channels. Now these channels are distinguished.

Flood channels: 1-9, 19-24, 26, 40-47, 50, 61-65, 74-81, 88, 108-110
Ebb channels: 11-16, 28-39, 54-58, 73, 91-105, 115-119, 183

The numbers are assigned as in Figure 2.1. The few remaining channels are relatively small and are neither ebb nor flood channels. For these channels the resistance is set independent on the direction of the flow. Now the variation of the resistance is applied with the right sign for the ebb channels and the flood channels.

Δ with a distinction between ebb and flood channels	V-T	T-H	H-B	B-A
run 12	3	2	8	2
run 13	5	5	5	5

Run 12 has the same Δ as run 11, which is the optimal run so far, but now Δ is applied with a different sign for ebb channels and flood channels. The average Δ of run 12 is equal to 5, which is used in run 13.

The residual discharge over a tidal period in the model is given in Figure 2.5. This has been compared to the residual discharge computed by the 2D DETWES model. The tidal volumes for the Pass of Terneuzen-Everingen have been of special interest in the calibration of the DETWES model. The volumes in the SOBEK computations are smaller, see Table 2.7, which is probably due to a different boundary condition (average M_2-M_4 tide). The volumes for Everingen agree with the volumes found by DETWES, considering the differences in bathymetry and boundary conditions. The volumes for Terneuzen show less asymmetry than found by DETWES.

Table 2.7 Tidal volumes at Terneuzen-Everingen. For Everingen, the tidal volumes in branch 42-50-51 are added and for Terneuzen the volumes in branch 24-32 are added (see Figure 2.1).

volume 10^6 m^3	run 12		run 13		DETWES	
	flood	ebb	flood	ebb	flood	ebb
Terneuzen	259	315	253	335	293	412
Everingen	496	449	515	426	597	501

The values for of run 12 show a circulation of approximately 50 10^6 m^3 per tidal period. This is less than the circulation in the DETWES model, which is approximately 100 10^6 m^3 per tidal period. The total tidal volume in run 12 is also less than the tidal volume in DETWES, but this may be explained by the fact that the cross section for which the tidal volumes were computed in the DETWES model does not coincide with the cross section in SOBEK. The circulation can be increased by increasing the asymmetry for Everingen-Terneuzen, as is done in run 13. The circulation increases to approximately 85 10^6 m^3 per tidal period.

In run 13 the circulation is improved. This run is the final result of the step by step calibration of the tidal harmonics. Now it has to be checked that M_2 and M_4 are still of the right order.

Table 2.8 result of the final calibration for M_2 and M_4

The tidal harmonics in run 13		Vlissingen	Terneuzen	Bath	Antwerp
M_2	model real	1.75 59° 1.74 59°	1.86 71° 1.87 68°	2.04 93° 2.10 94°	1.80 128° 1.96 116°
M_4	model real	0.12 117° 0.13 117°	0.08 137° 0.12 133°	0.12 169° 0.12 167°	0.17 197° 0.13 179°

The model boundary is at Vlissingen, which therefore coincides well with the actual tide. Compared to the calibration on M_4, the relative error has increased at Terneuzen but it has decreased at Bath. At Antwerp, the relative error is large but it is slightly less than in the calibration on M_4.

The residual velocities are given in Figure 2.6 and are in the order of 0.1 m/s which is the same order as in DETWES. The direction of these 1D computations agrees with the DETWES results, although there are differences at the sea boundary. This may be explained by a difference of the boundary conditions (the EENDMORF model uses a simplified M_2-M_4 boundary). The global circulation patterns are similar.

For the parameters in run 13, the relative error as given by equation (2-4) is in the order of 10%, if it is assumed that the amplitude of the velocity is proportional to the amplitude of the water level.

2.7 A comparison of IMPLIC and SOBEK for the re-calibrated flow

The re-calibration of the flow is carried out to minimise the term (2-3). The re-calibration gives a flow which is different from the original flow in the IMPLIC model. The velocities of the tidal flow in IMPLIC are compared to the velocities in the recalibrated model, see Figure 2.7. There is a relatively large difference. The velocity is smaller in the re-calibrated SOBEK model because it uses a different boundary condition, as discussed in section 2.2, and because the tidal amplitude is smaller between Bath and Antwerp. On average, the velocities are reduced by 20% after the recalibration. The amplitude of the M_2M_4 tide is approximately 15% smaller than the amplitude of the average tide, see section 2.2, so the main cause for the lower velocity is the different boundary condition. In the simulation of the sediment transport and the morphological development, both the average tide and the M_2M_4 tide are used.

2.8 Conclusions

The water flow has been re-calibrated, minimising the term given by equation (2-4) for the relative error. The only parameter to calibrate the flow is friction, which has been varied to calibrate first M_2 then M_4 and finally M_0.

The following can be concluded:

1. The original parameters of the IMPLIC model give good results for M_2 and M_4 for the stations Terneuzen and Bath. At Antwerp, the amplitude is too large. By increasing the friction between Bath and Antwerp, the model results were improved.

2. The circulation of the residual flow (M_0) in the model is comparable to the circulation in the 2D model DETWES.

3. The relative error for the sediment transport (2-4) has been minimised to 10%, under the assumption that the amplitude of the water level is proportional to the amplitude of the velocity.

4. The boundary condition which is used in the calibration is an M_2M_4 tide so there is no interference of other harmonics. It has an amplitude which is smaller than the amplitude of the average tide at Vlissingen. Because of this smaller amplitude, the velocities as found in the calibration are smaller than the velocities in the original IMPLIC model. In the simulations of the next two chapters, both boundary conditions are used to study the dependence of the boundary conditions.

5. If the parameters are set equal, the SOBEK results are almost equal to the IMPLIC results. There is a small difference which is probably due to the fact that IMPLIC uses the hydraulic radius as an extra input parameter and SOBEK does not.

3 The sediment transport

The sediment transport in the model is computed from the Engelund-Hansen transport formula, which depends on the flow velocity. In the original formula, the transport coefficient depends on the friction parameter. In the Westerschelde model, however, this parameter is used as the single calibration parameter. Therefore, the friction parameter is not used in the transport formula. The transport coefficient in the Engelund-Hansen formula is computed for a constant Chézy coefficient of 45 $m^{0.5}/s$.

The simulations are carried out with an M_2M_4 boundary condition as well as an average tide. The M_2M_4 is adapted to include the average effect of the semi-diurnal S_2 component, which has an amplitude of 25% of M_2. The amplitude of M_2 is increased by 12%.

This chapter is divided as follows. First it is considered if the model is more or less in morphological equilibrium. Then the circulation pattern of the sediment transport is exhibited. The simulated sediment transport is compared to measurements in nature, as processed by Van Kerckhoven (1995). Finally, the sand balance of the model is checked.

3.1 The transport coefficient

For river flow in a single channel, a morphological equilibrium is reached if the flow velocity is constant, i.e., if Q/A is constant. Wang (1995) has used this to give an analogous relation for a morphological equilibrium in a single channel estuary:

$$\frac{BMV^5}{A^5} = \text{constant} \qquad (3\text{-}1)$$

M	= transport coefficient	$[s^4/m^3]$
A	= area of the cross-section	$[m^2]$
B	= sediment transport width	$[m]$
V	= tidal volume	$[m^3]$

There are two morphological parameters in this equation: the transport coefficient M and the sediment transport width B_s. The value of the ratio (3-1) is computed for various cross sections of the Westerschelde, shown in Figure 3.1. The value for B is computed by adding B's of model branches.

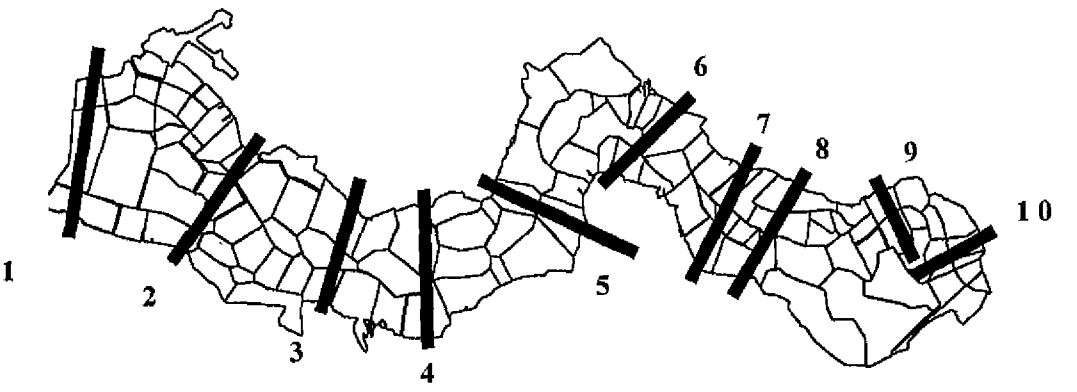

Figure 3.1 ten cross sections to compute the constant (4)

The values of the ratio (3-1) are given in Figure 3.2. For the major part of the Westerschelde it is more or less constant, with variations in the order of a factor 2. So, the Westerschelde model is close to a morphological equilibrium. This agrees with the fact that dredging and dumping activities in the estuary were relatively minor before 1968.

The only significant variation of the ratio (3-1) occurs for sections 8, 9 and 10 located in the eastern part of the estuary. This is also the part of the model where the flow is the hardest to calibrate. So the variation may be due to problems to simulate the flow or it may be due to the morphological activity in the eastern part of the Westerschelde.

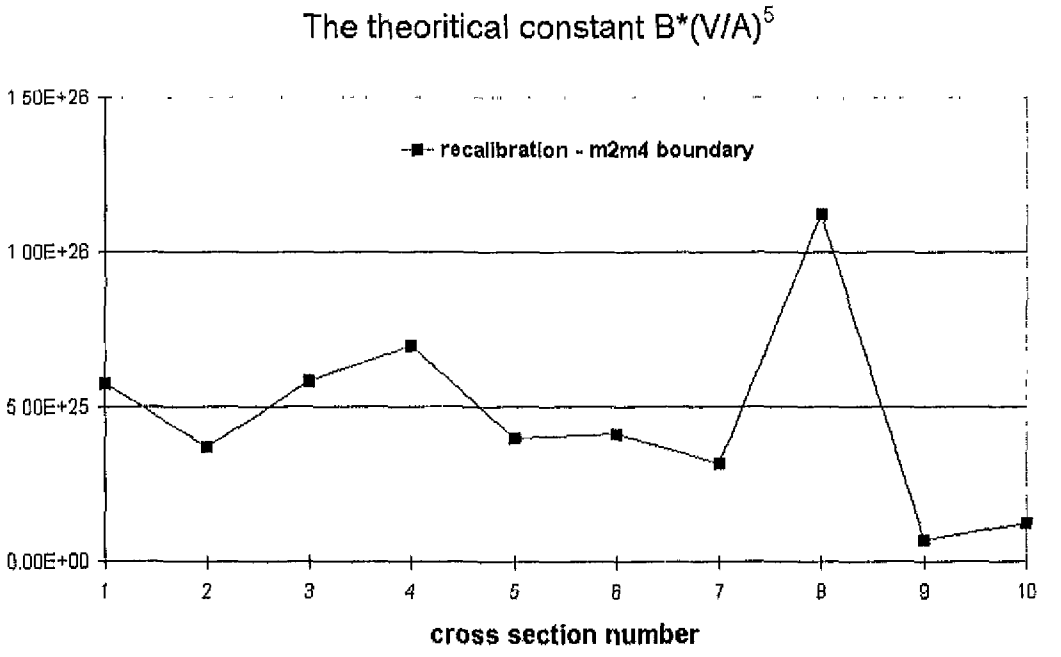

Figure 3.2 The ratio (3-1) for the 10 cross sections of Figure 3.1

The quotient is computed for different simulations to study the irregularity of (3-1) for the eastern part of the estuary. These simulations are: a simulation with the original IMPLIC parameters and a simulation with the average tide such as used in the ESTMORF model. The results are shown in Figure 3.3.

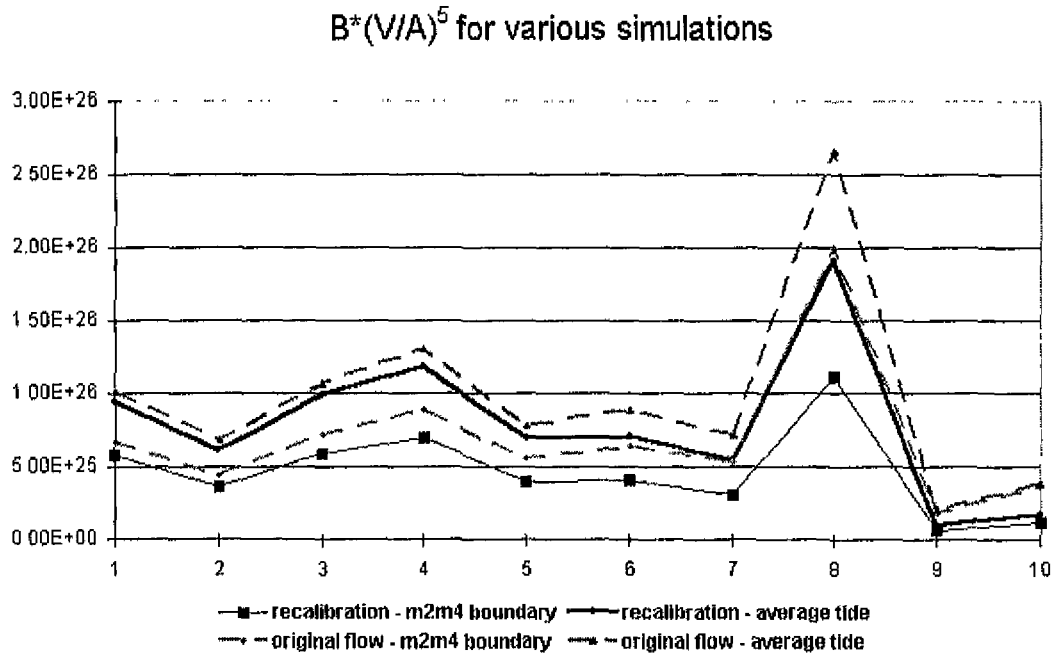

Figure 3.3 The quotient (3-1) under the variation of friction and boundary conditions

The following can be concluded from this figure:

1. The ratio shows the least variations for the re-calibrated flow. So, the recalibration gives a model which is closer to a morphological equilibrium.
2. The ratio is larger for the average tide, because of the larger tidal range. For this boundary condition, the morphological response to interference is faster.
3. Apart from the difference in magnitude, the two different boundary conditions give a similar result for the ratio (3-1). So, apart from a difference of time scales, the two boundary conditions should give a similar morphological response.

These conclusions can be verified for the morphological evolution as simulated in the next chapter.

3.2 The sediment transport field

The sediment transport is simulated for the two different boundary conditions. For both boundary conditions, the sediment transport field is shown in Figure 3.4 and 3.5 below.

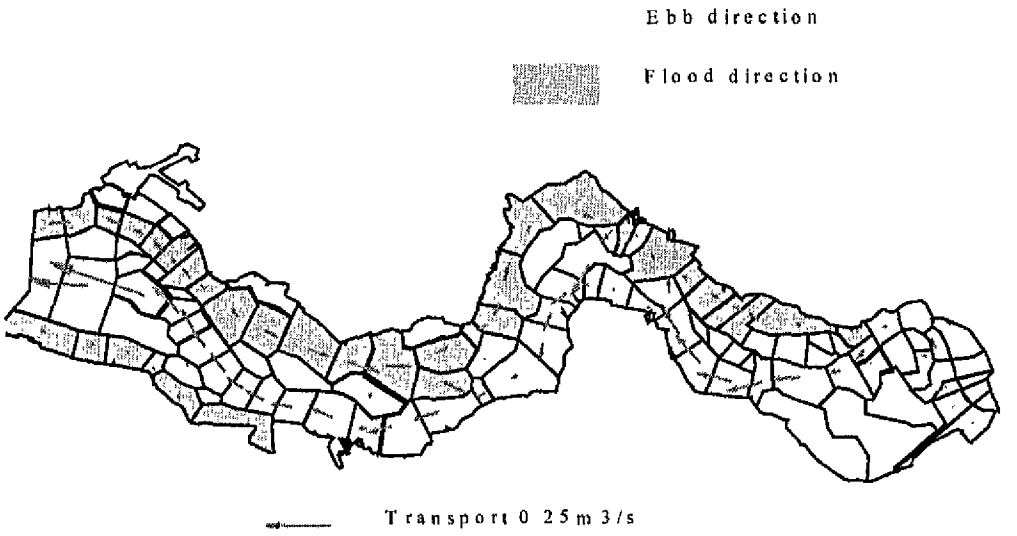

Figure 3.4 The sediment transport field for the M_2M_4 boundary condition

The dark shaded areas are the flood channels and the light shaded areas are the ebb channels.

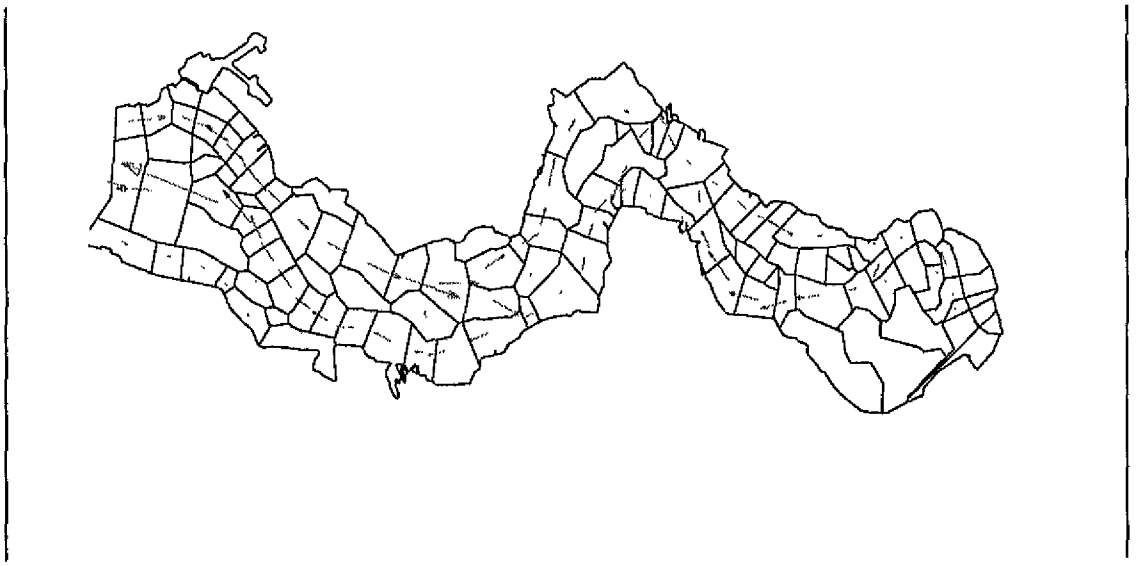

Figure 3.5 The sediment transport field for the boundary condition of an average tide.

The differences between these transport fields is relatively small. Both boundary conditions give the same circulation pattern of the sediment transport field. This pattern is the same as the circulation pattern of the residual flow. There are roughly three circulating cells: between Vlissingen and Terneuzen, between Terneuzen and Hansweert, between Hansweert and Bath.

The quotient (3-1) considers entire cross sections only. The circulation pattern gives information of individual channels. For the M_2M_4 boundary condition the transports in the flood channels are slightly smaller than the transports in the ebb channels. For the average tide the sediment transports in the flood channels are as large as the sediment transports in the ebb channels. So, for the M_2M_4 boundary, sedimentation can be expected in the flood channels, while erosion can be expected in the flood channels. For the average tide, the model can be expected to be closer to a morphological equilibrium.

The sediment transport is calibrated on data of the Pass of Terneuzen-Everingen. The measured sediment transports in various measuring points over the cross section were integrated in a previous study (Van Kerckhoven, 1995) and are given in Table 3.1. These estimates indicate that the residual transport over the entire cross section of flood channel and ebb channel is flood dominated.

Table 3.1 estimated sediment transports

	OBSERVED DATA			MODEL	
estimated transport	ebb transport	flood transport	residual transport	residual transport M_2M_4 boundary	residual transport average tide
Terneuzen	0.39 m^3/s	0.27 m^3/s	-0.12 m^3/s	-0.16 m^3/s	-0.09 m^3/s
Everingen	0.32 m^3/s	0.51 m^3/s	+0.19 m^3/s	+0.09 m^3/s	+0.12 m^3/s

Considering that the data have a large incertainty, both results are close to the data. The results of the average tide are relatively in better agreement than the results of the M_2M_4 boundary condition.

3.3 The sand balance

The sediment transport model is checked by a sand balance. In each model branch, the inward transports, the outward transports and the bed level changes should add up to zero. This has been checked for all branches in the model and the balance closes. The balance is shown in Figure 3.6 for the model balance of branches with the largest sedimentation.

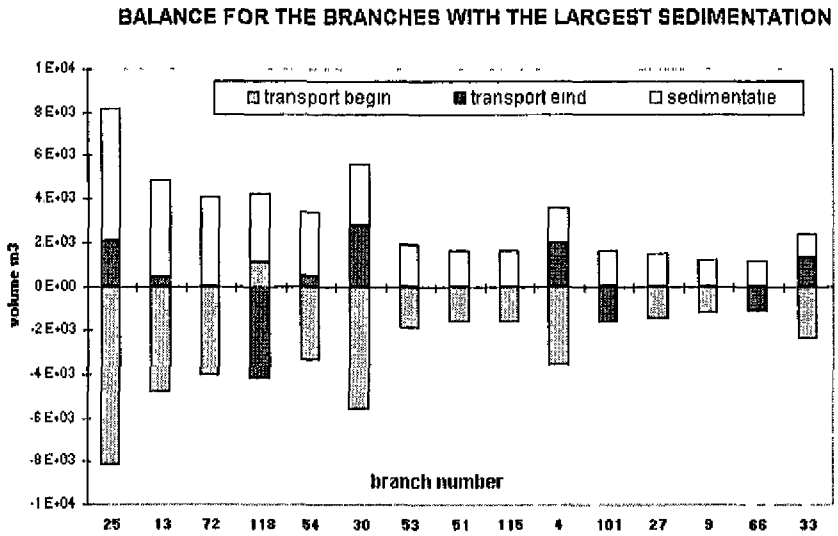

Figure 3.6 sand balance for the branches with the largest sedimentation in the model

The following comment should be made. SOBEK uses a correction term on the sediment transport to get a higher order numerical scheme. The transports in Figure 3.6 are the transports with the correction term. In some of the branches, this correction term is as large as the computed sediment transports . The sand balance for the sediment transports without the correction term does not close for these branches.

The sand balance for large regions of the Westerschelde shows that there is a net erosion, contrary to the sedimentation which is found in the mass balance of Uit den Boogaard. In Figure 3.6 the yearly erosion in the model is given for the Westerschelde divided into 5 large regions, at intervals of 10 km from Vlissingen to the Belgian border. The results are given for the two different boundary conditions.

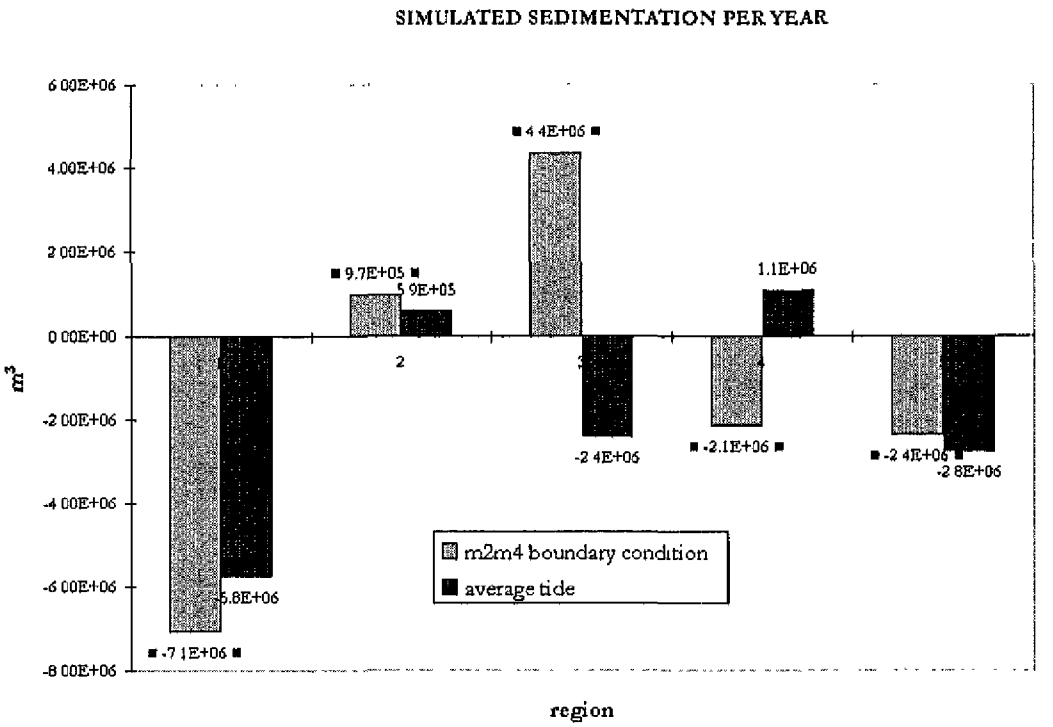

Figure 3.7 sand balance for 5 regions of the Westerschelde (1=Vlissingen, 5=border)

The yearly erosion in the model is approximately 5 10^6 m^3/year whereas the required maintenance dredging is approximately 4 10^6 m^3/year during the period 1965-70 (Uit den Boogaard, 1995). There is also a difference between the boundary conditions, in particular for regions 3 and 4.

These results show that the sediment transports at the model boundary is not yet accurate. The erosion in the modek, which does not agree with the observed sedimentation in the Westerscheld, is due to the model schematisation at the sea boundary. This is discussed in the next chapter.

3.4 Conclusions

1. The simulated sediment transport shows the same circulation patterns as the residual flow. It agrees well with measured data as processed by Van Kerckhoven (1995).
2. The quotient which indicates whether a one-channel model is in equilibrium, derived by Wang (1995), is more or less constant for the largest part of the estuary. Only the eastern part of the estuary shows a variation of the quotient.
3. The average tide gives a sediment transport field which is smoother than the M_2M_4 boundary condition. Under the latter condition, the transports in the flood channel are lower than the transports in the ebb channel.
4. The sand balance shows that there is erosion in the model, while sedimentation is observed in nature.

4 The morphological evolution

Human interference has a large impact on the morphological evolution of the Westerschelde. After 1968 the dredging operations were increased to deepen the channels in the estuary. The model areas with the largest interference are shown in Figure 4.1.

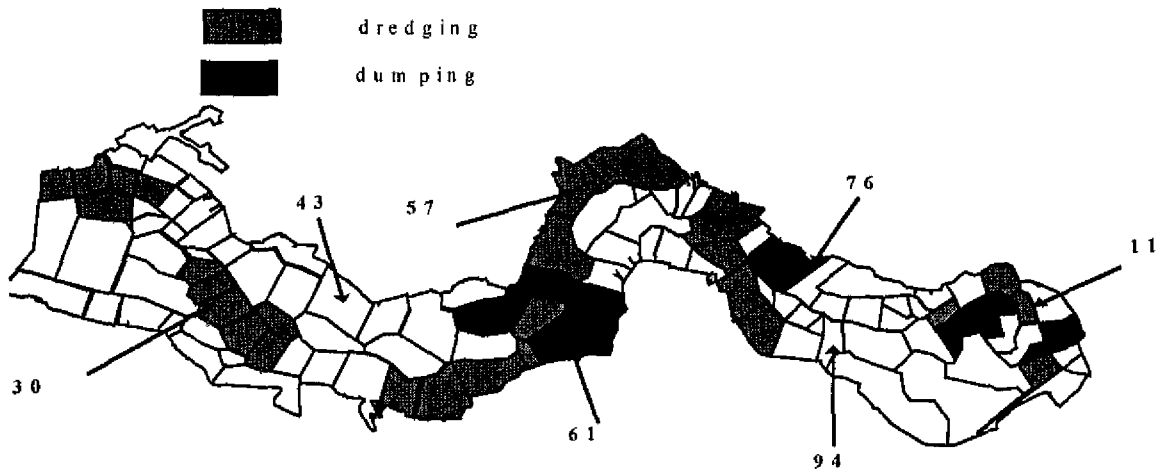

This chapter contains simulations of the morphological development of the Westerschelde over the period 1968-78. The human interference in this period has been modelled as a continuous process. The following simulations have been made:

Table 5.1 description of the model computations

scenario	description
1	The morphological development without dredging and dumping for the M_2M_4 boundary condition.
2	The morphological development with dredging and dumping for the M_2M_4 boundary condition.
3	The morphological development without dredging and dumping for the average tide.
4	The morphological development with dredging and dumping for the average tide.
5	The morphological development with dredging and dumping for the M_2M_4 boundary condition, varying the exponent of the nodal point relation.

The model results are compared to establish the influence of the boundary condition, the dredging and dumping activities and the nodal point relation.

4.1 The influence of the boundary condition

The evolution of the volume of 6 model branches is shown in Figure 4.2. Each branch represents one of the main ebb channels or flood channels. The evolution is shown for the first 4 simulations, as well as the real evolution (as measured in 1967, 1971, 1973 and 1977) and the volume changes due to human interference. The human interference is modelled as a continuous process.

There is a clear difference between the boundary conditions for the ebb channel/flood channel between Hansweert and Bath (branch 76 and 94). The average tide gives that the ebb channel is more or less stable, while the flood channel erodes. The M_2M_4 tide gives erosion in the ebb channel and sedimentation in the flood channel. In this respect, the results for the average tide are in better agreement with the measurements, which indicate that both the ebb channel and the flood channel are more or less stable.

The morphological evolution of the channels between Vlissingen-Terneuzen and Terneuzen-Hansweert is similar for both boundary conditions. There is a slight erosion in the ebb channel between Terneuzen and Hansweert while there is sedimentation in the flood channel. Both the ebb channel and the flood channel between Vlissingen and Terneuzen erode in the model simulations. The model results agree with the measurements for the ebb channel/flood channel between Terneuzen and Hansweert. The model results do not agree for the ebb channel/flood channel between Vlissingen and Terneuzen, which is stable according to the measurements, while there is erosion in the model.

Figure 4.3 The model boundary

The erosion between Vlissingen and Hansweert is due to a net sediment transport out of the estuary (as shown in the sketch of the model boundary, Figure 4.3). At the model boundary, the sediment transport in the ebb channel is directed outward, while the transport in the flood channel is directed inward. The transport in the ebb channel increases during the simulation, while the transport in the flood channel remains almost constant. In the current layout of the model, the transport out of the ebb channel cannot be directed into the flood channel. The model results may improve if the model network is adjusted.

For all branches in Figure 4.2, the model results shows a sand wave. The model develops towards a morphological equilibrium which is different from the initial bathymetry.

4.2 The influence of the dredging/dumping activities

In the model, the volume changes due to human interference are smaller than the volume changes due to natural development. As Figure 4.2 shows, the difference between scenario 1 and 2, as well as the difference between scenario 3 and 4 is relatively small. The different boundary conditions have a larger impact than the human interference.

Model branch 115 located in the ebb channel in front of Bath (see Figure 4.1) has the largest human interference. It is being dredged. This model branch has been used in the ESTMORF simulations to calibrate the morphological time scale. Both scenario 1 and 3 show a natural erosion of the branch. The impact of the dredging as simulated by the model is 10^7 m^3 for the M_2M_4 boundary condition, i.e., scenario 2 - scenario 1. It is 0.9 10^7 m^3 for the average tide, i.e., scenario 4 - scenario 3. The dredged volume is 1.3 10^7 m^3 and the measured volume increase is 0.4 10^7 m^3. The model therefore simulates a response slower than nature, but this may be explained by the natural erosion of the branch in the model.

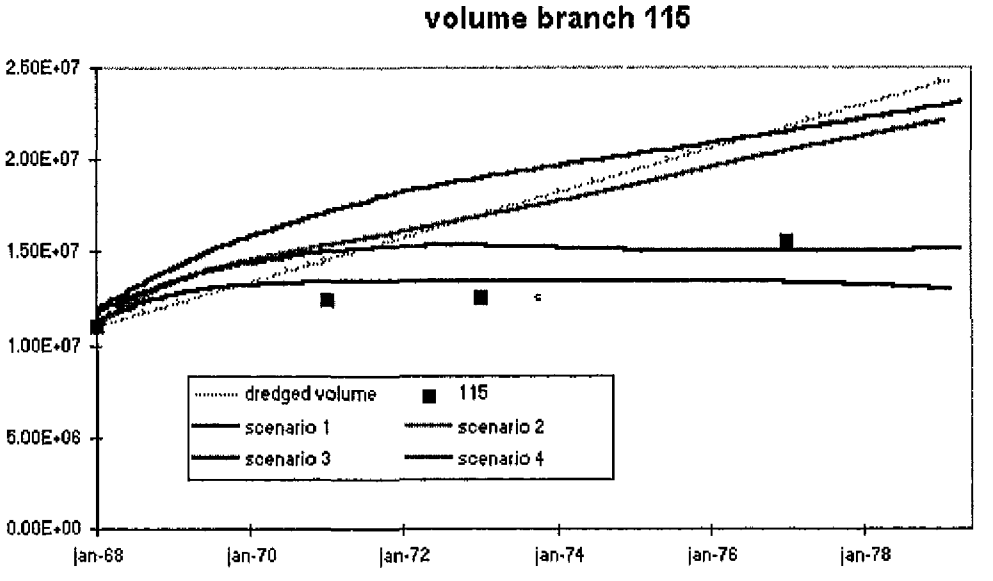

Figure 4.4 The evolution of branch 115

The computation for branch 115 can also be made for the entire area where there is dredging (dumping). For the area where there is dredging (dumping) during 1968-78, the total volume can be compared to the total volume change in the scenario's minus the natural development.

Table 5.2: The total effect of dredging and dumping

activity	volume (per year)	volume for average tide	volume for M_2M_4 boundary
dredging	7.3 million m^3	3.5 million m^3	4.7 million m^3
dumping	1.6 million m^3	0.4 million m^3	0.2 million m^3

For both boundary conditions, the dumped volume has almost disappeared, while the dredged volume is decreased by 50%. In contrast, according to the data of the period 1968-78, the dredging operations maintain the channel volume but do not increase it. So the dredged and dumped volumes are re-distributed. The model does not show this behaviour because its natural development is to erode. The model results may improve if its natural development is improved.

4.3 The influence of the nodal point relation

The nodal point relation controls the long term morphological development of the model, see (Wang et al, 1994). The exponent of the nodal point relation influences the morphological time scale and the morphological equilibrium. For an exponent greater than 5/3 the channels are morphologically stable, for an exponent smaller than 5/3 the channels are morphologically unstable. In the simulations 1, 2, 4 and 5 the exponent is 3 for each node in the model. The nodal point relation is used to get stable channels.

The sediment transport field in the Westerschelde consists of three circulation cells, see Figure 3.4 and 3.5. Each cell consists of an ebb channel and a flood channel. In simulation 3, the exponent is set 1 for the nodes which connect the ebb channel to the flood channel.

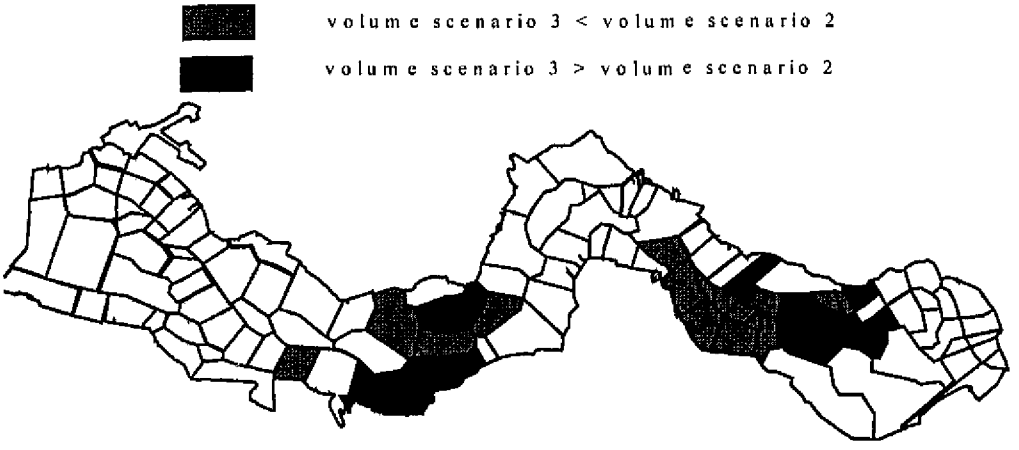

Figure 4.3 The influence of the nodal point relation

The influence of the nodal point relation is shown in Figure 4.3. It has some effect, especially on the ebb/flood channel between Hansweert and Bath, but the volume changes are relatively minor. The branches 81, 87, 88 and 90, which are small branches outside the main channels, are the only ones with significantly different volumes. The order of the difference between simulation 2 and 3 is 25%. So the influence of the nodal point relation on the time scale of 10 years is relatively small.

4.4 Conclusions

1. The model simulations show erosion in the western part of the model. This is probably caused by the layout of the model network at the boundary. The network layout may be adapted to improve the model results in the future.

2. The simulated morphological evolution shows the same trend as the data for the area east of Terneuzen.

3. The impact of dredging and dumping has been simulated, by comparing simulations with interference to simulations without human interference (natural development). The results may be improved if the simulation of the natural evolution is improved (conclusion (1)).

4. The nodal point relation has only a minor influence on the model results over the period 1968-78. In the model, the nodal point relation has only been used to get a morphologically stable evolution.

5 Summary

The present study is one in a series of EENDMORF studies. Previously, it has been studied how to obtain a stable model behaviour through nodal point relations and how to calibrate the tidal harmonics through the variation of the resistance with the direction of the flow. The present study is the first step to an operational network morphodynamic model of the Westerschelde.

The water flow in the model has been calibrated for morphological purposes. The harmonic constituents of the tide have been calibrated one by one by varying the friction parameter, to minimise the relative error of the sediment transport. The circulation of the residual flow and the residual sediment transport, which are characteristic for the estuary, are reproduced by the model.

The calibrated model has been used to simulate the morphological development of the Westerschelde over the period 1968-78. The model results show the same trend as the measurements for the eastern part of the estuary. For the western part of the estuary, the model shows erosion while in reality the channels there are in relative equilibrium. This model behaviour can be improved in future studies by adapting the schematisation at the model boundary.

References

L.A. uit den Boogaard, *Resultaten Zandbalans Westerschelde,* Rapport R95-08, IMAU, Universiteit van Utrecht, 1995.

R.J. Fokkink, *Simulations of estuarine morphology in simple network systems,* DELFT HYDRAULICS, report Z855, 1995.

K. de Jong and A.W. Heemink, *A study of a numerical tidally averaged morphodynamic model,* Delft University, Faculty of Mathematics, Report in preparation, 1996.

B. Karssen and Z.B. Wang, *Morphological modelling in estuaries and tidal inlets. Part I: a literature survey,* DELFT HYDRAULICS, report Z473, Delft, 1991.

J.D.M. van Kerckhoven, *Morphological modelling of ebb and flood channel systems in estuaries,* Masters Thesis, Delft University, Faculty of Civil Engineering, 1995.

J. van de Kreeke and K. Robaczewska, *Tide induced residual transport of coarse sediment; application to the ems estuary,* Neth. J. Sea Res. 31 (3), 1993.

Van de Male, K., werkdocument 2D model DETWES, Rijkswaterstaat, 1992.

Z.B. Wang, *About the schematisation of the geometry in a 1D morpodynamic model and the effect of narrowing on the morphological development,* DELFT HYDRAULICS, note, 1995.

Z.B. Wang, R.J. Fokkink, M. de Vries, A. Langerak, *Stability of river bifurcations in 1D morphodynamic models* , J. Hydr. Res., vol 33, no. 4, 1995.

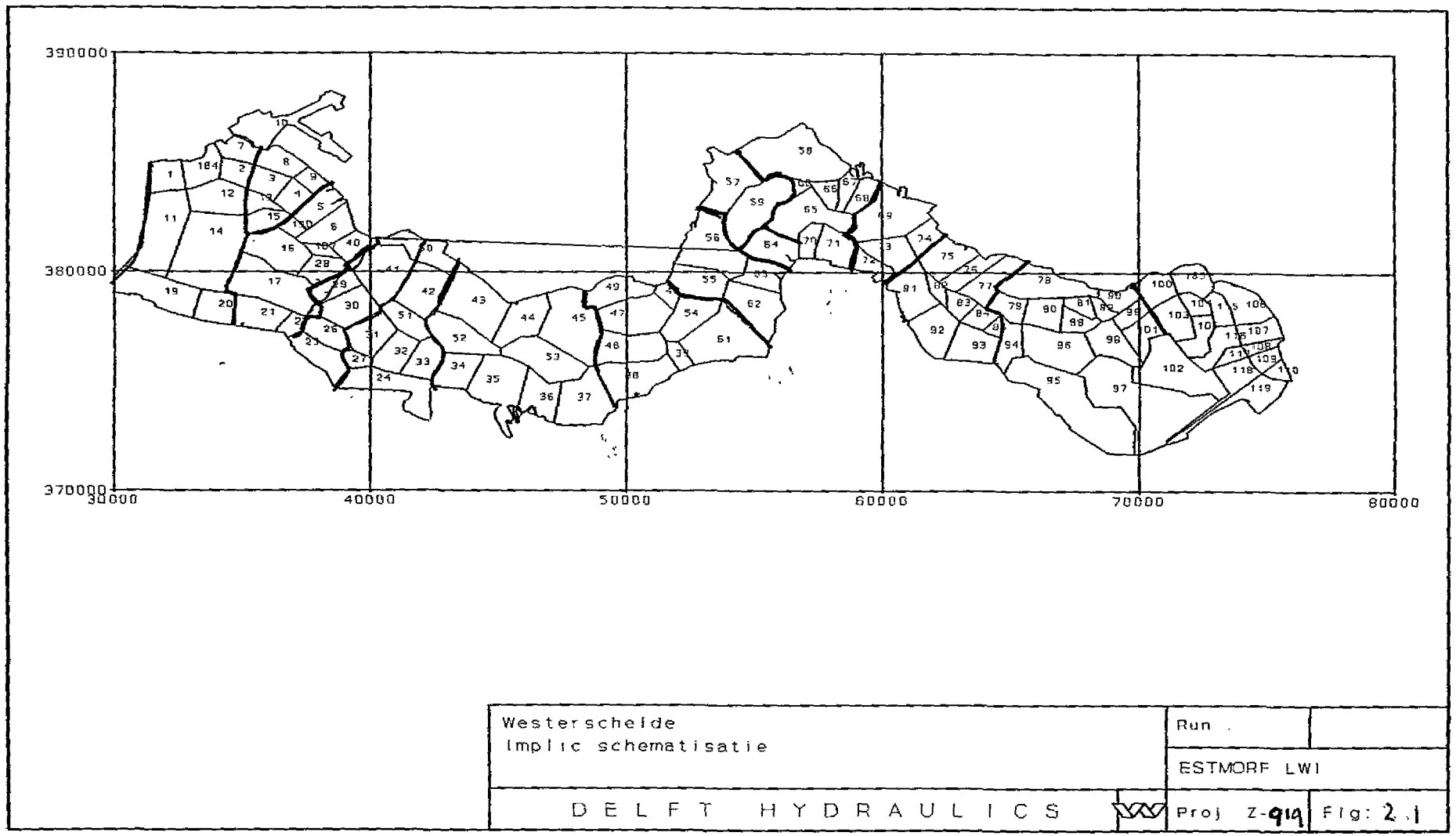
390000
380000
370000
30000
40000
50000
60000
70000
80000
Westerschelde
Implic schematisatie
Run .
ESTMORF LW1
DELFT HYDRAULICS
Proj Z-919
Fig: 2.1

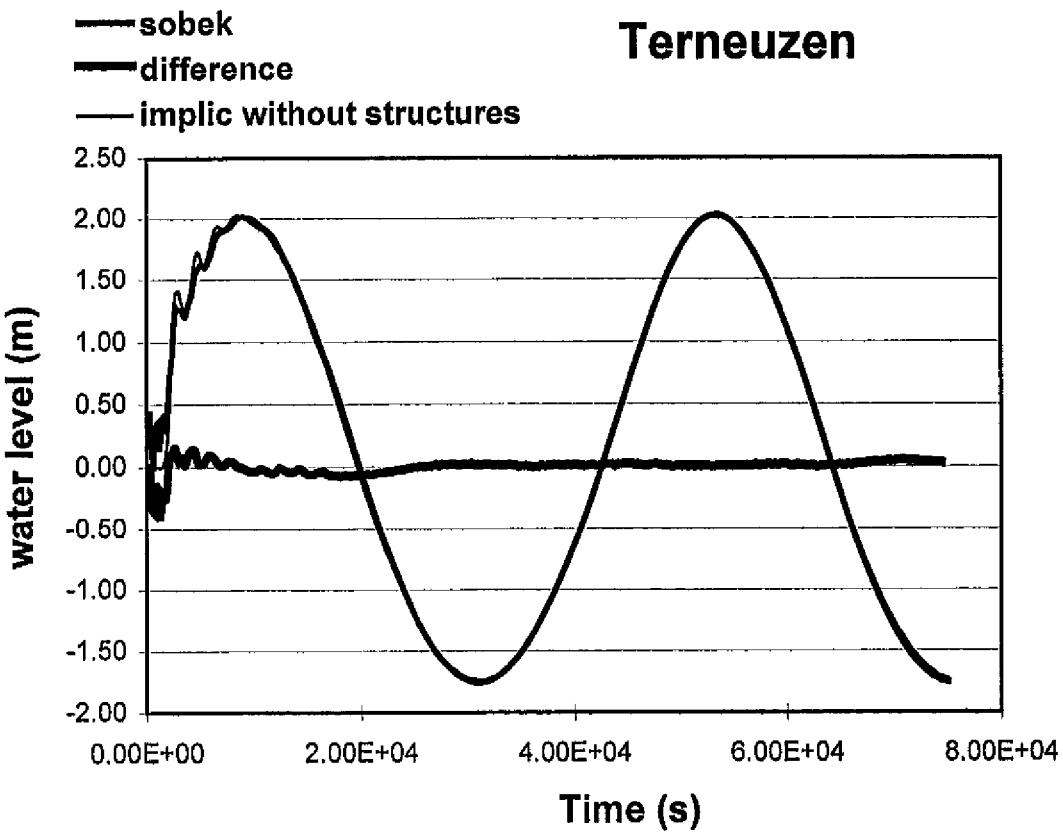

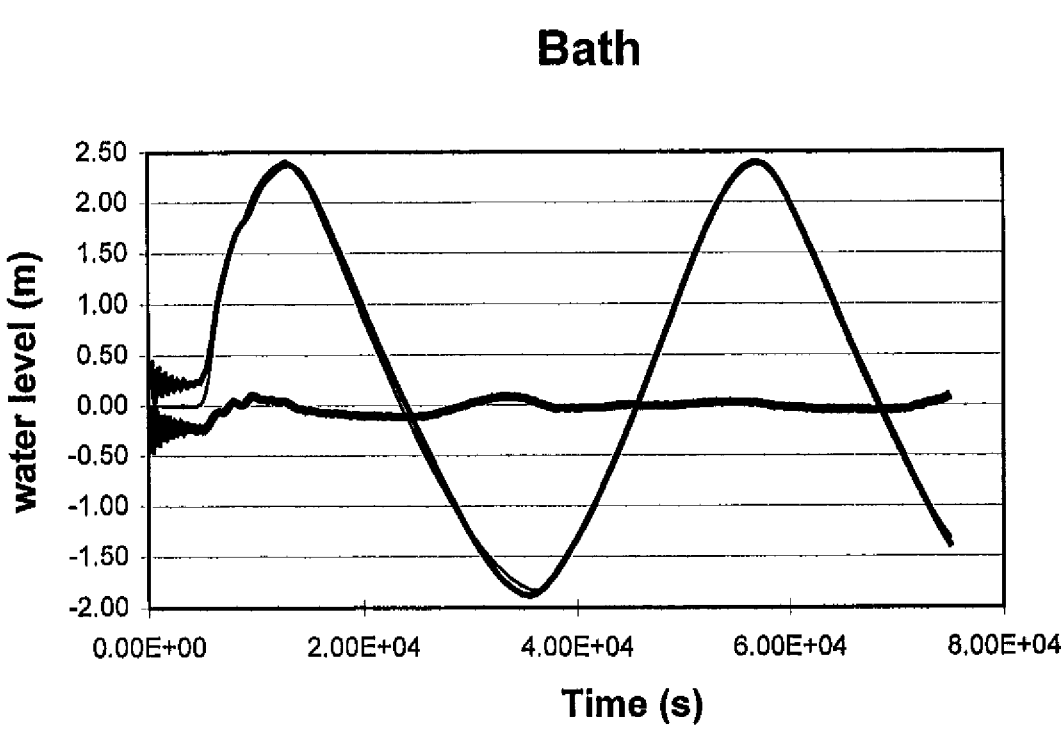

Water level in IMPLIC and in the transcription to SOBEK. No structures	Z919
DELFT HYDRAULICS	Figure 2.2

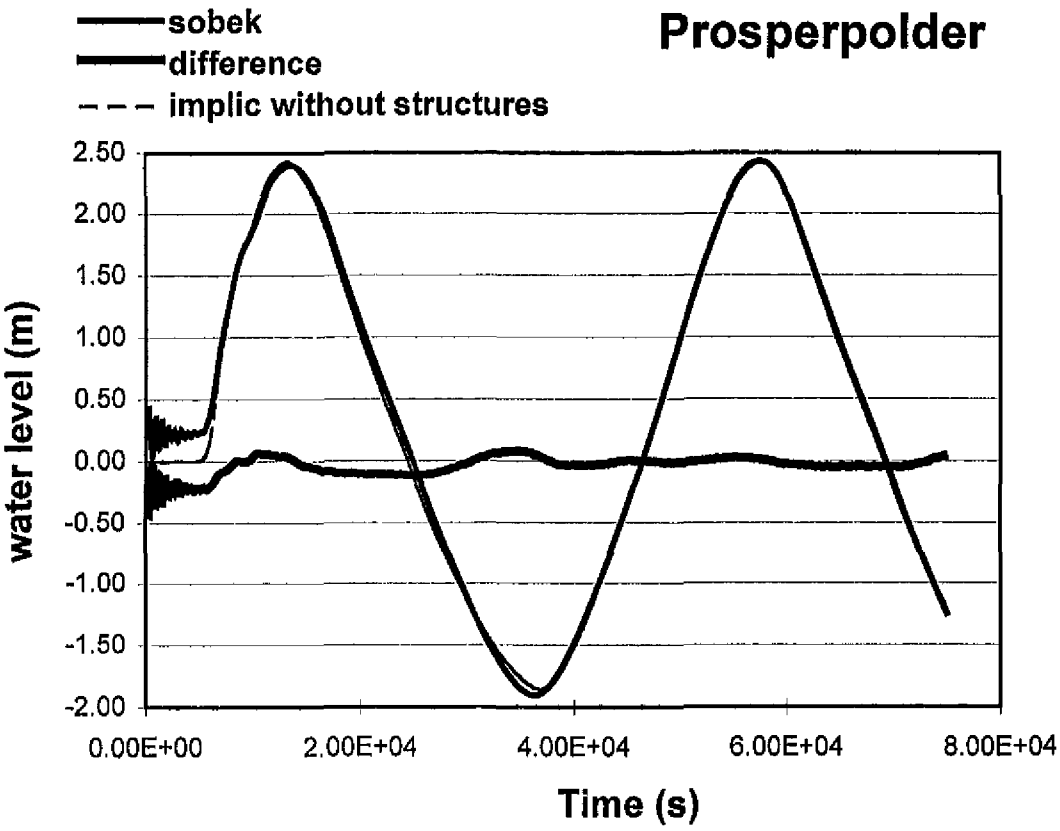

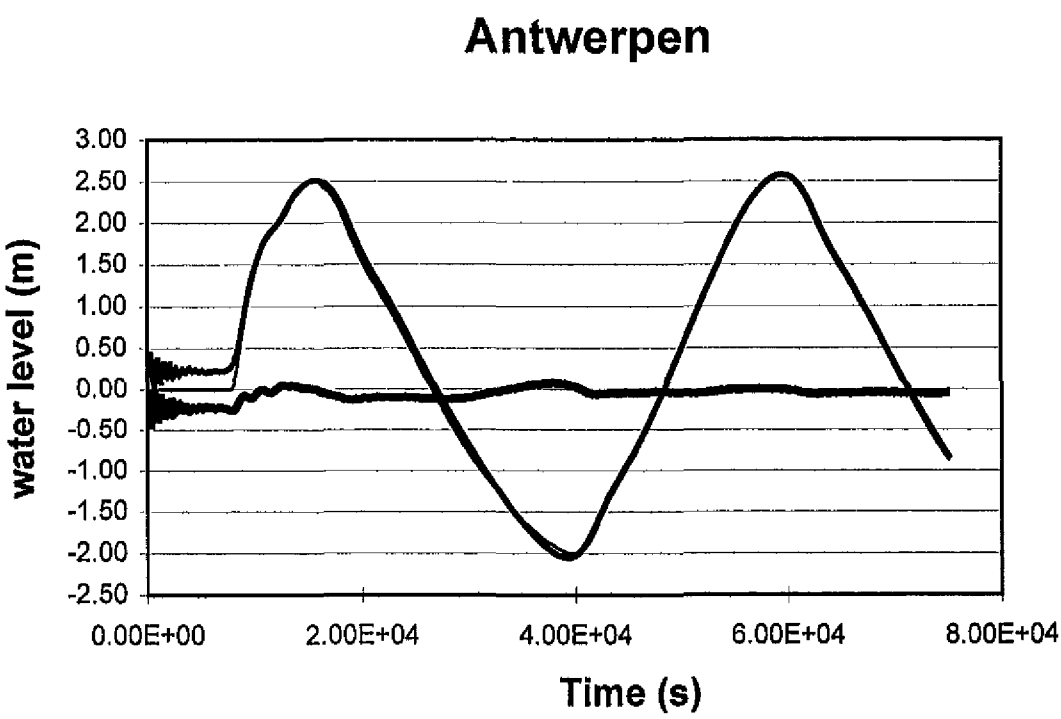

Water level in IMPLIC and in the transcription to SOBEK . No structures	Z919
DELFT HYDRAULICS	Figure 2.2

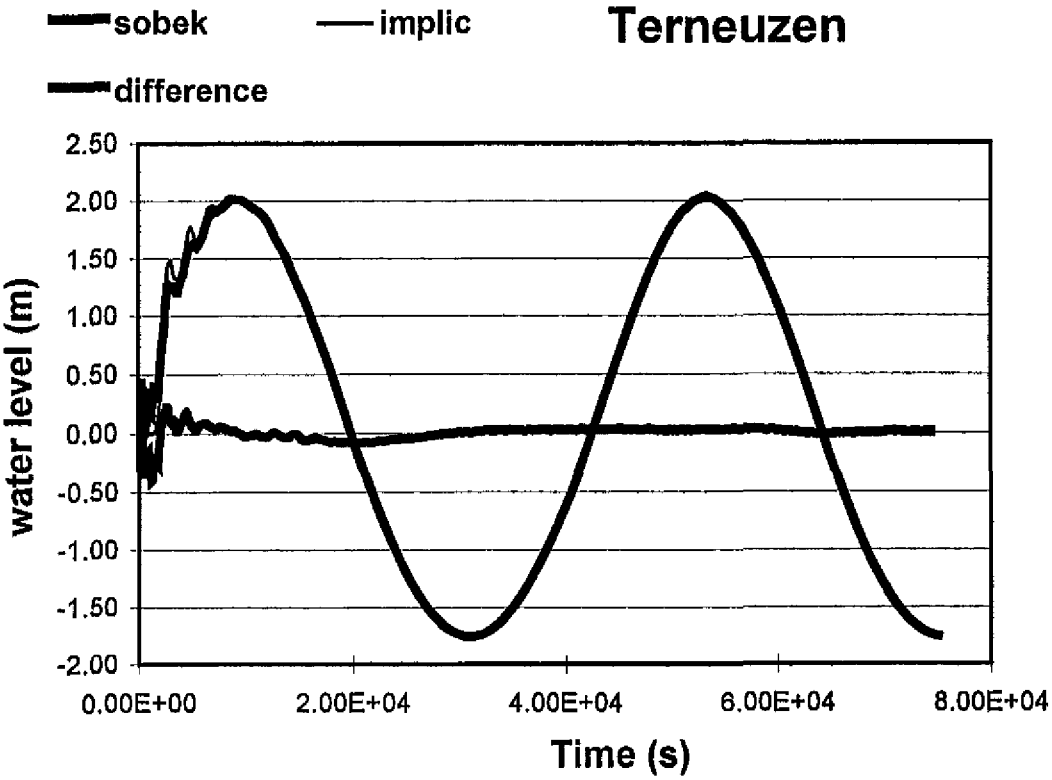

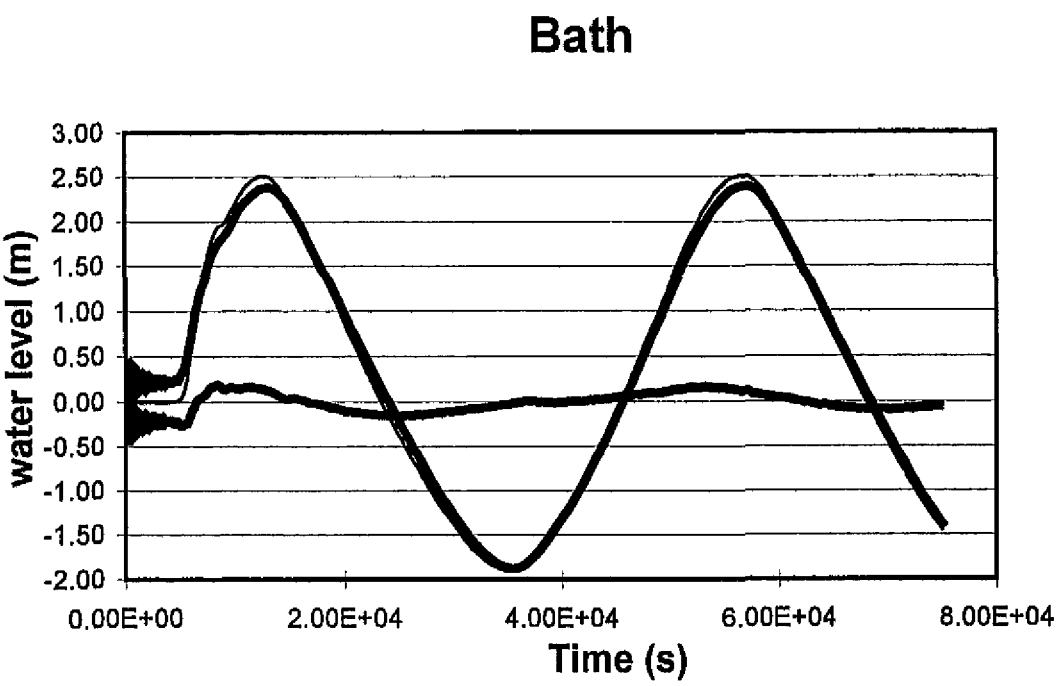

Water level in IMPLIC and in the transcription to SOBEK. IMPLIC with structures	Z919
DELFT HYDRAULICS	Figure 2.3

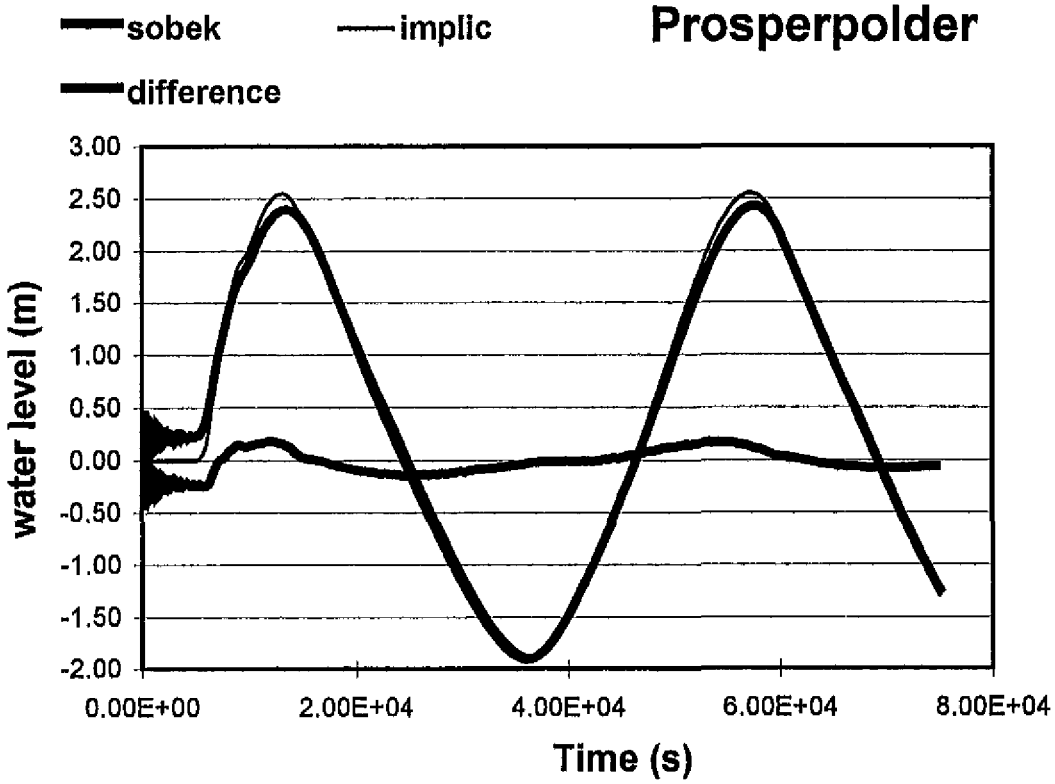

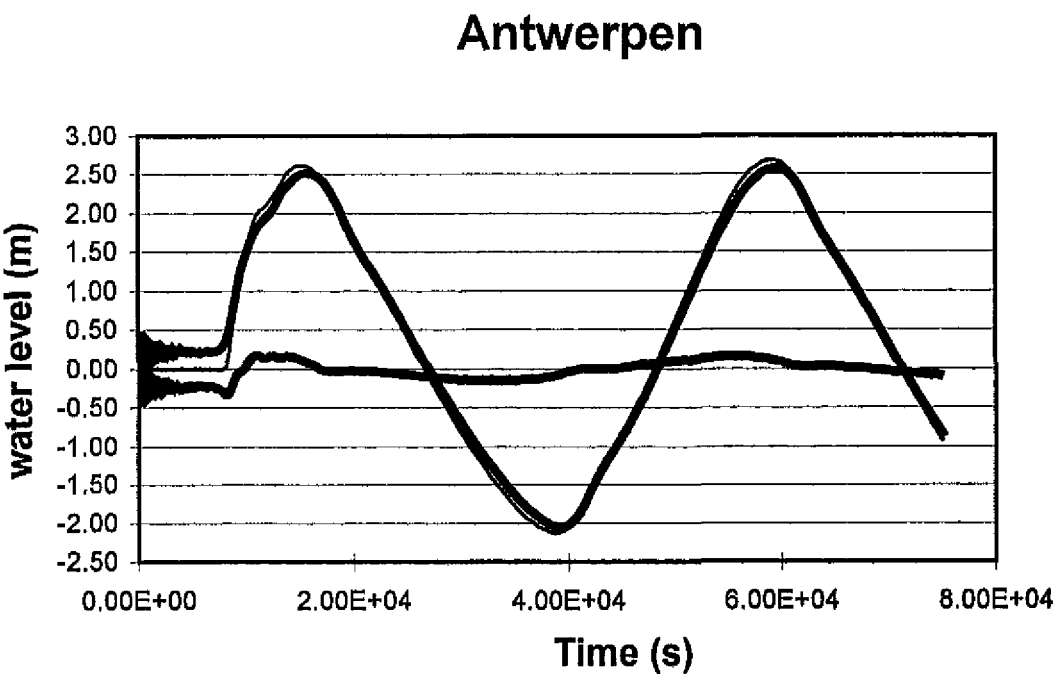

Water level in IMPLIC and in the transcription to SOBEK . IMPLIC with structures	Z919
DELFT HYDRAULICS	Figure 2.3

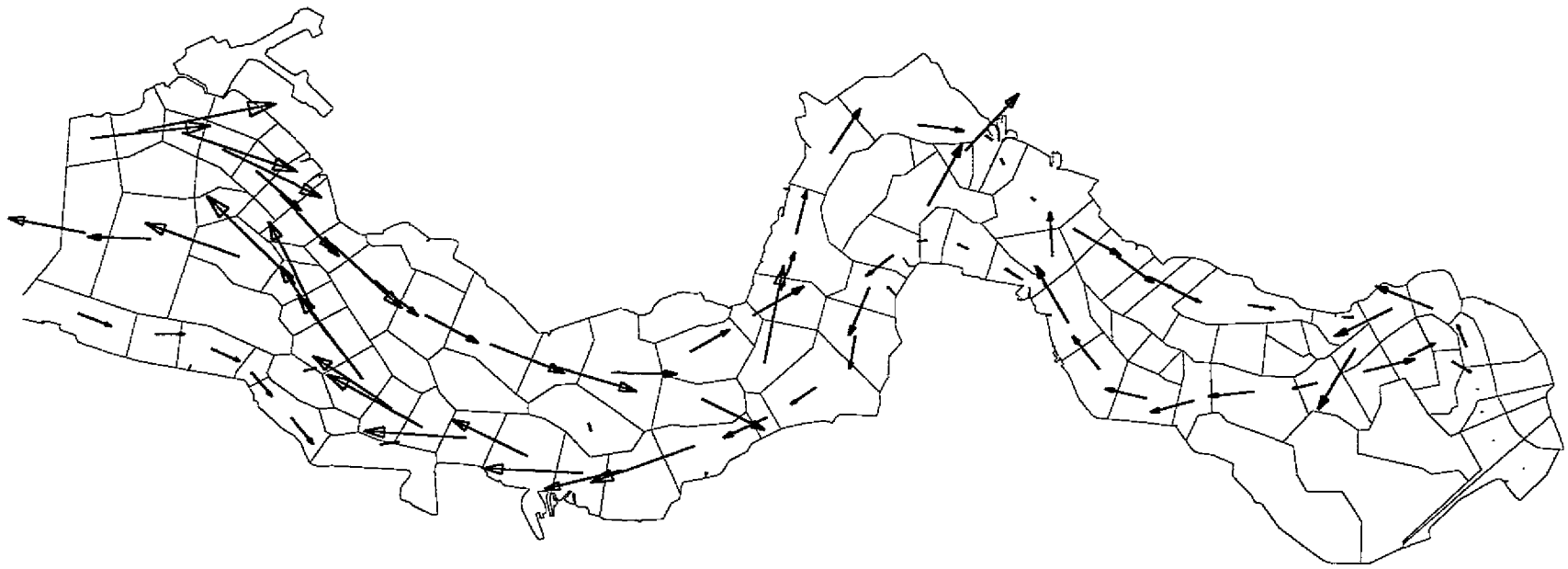

2. m2/s

Westerschelde
specific discharge over a tidal period
test

DELFT HYDRAULICS

Fig 2.5

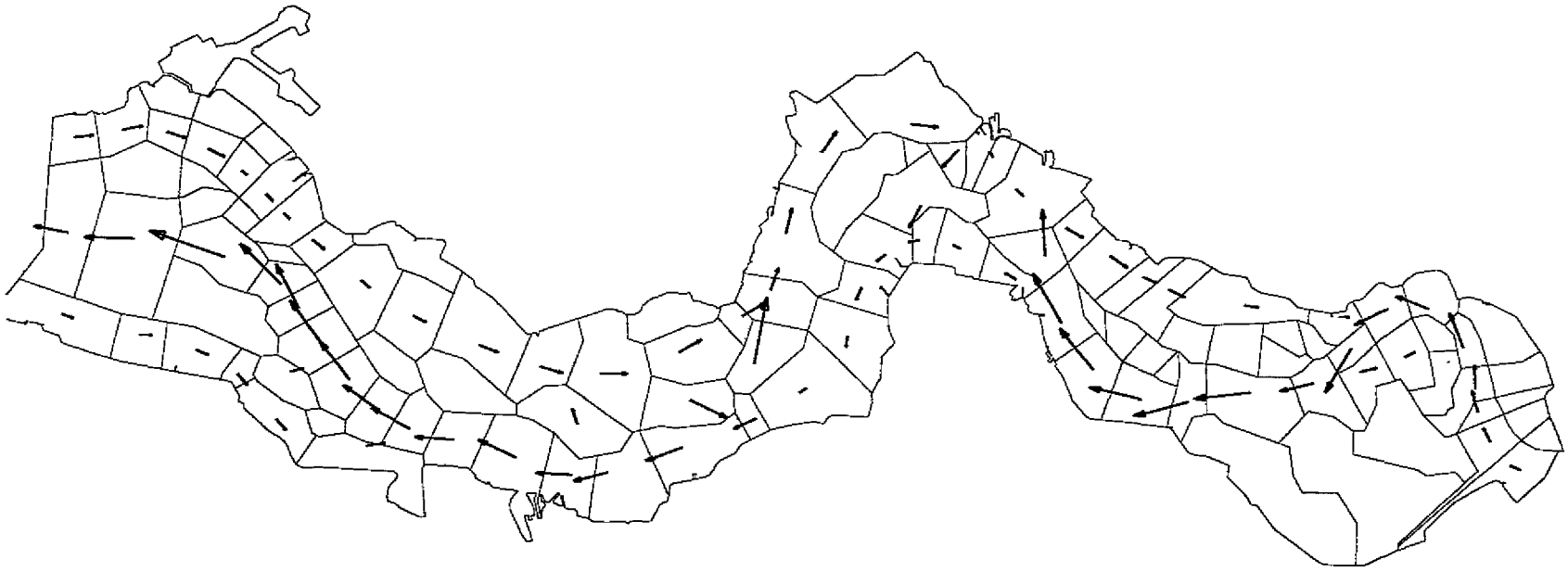

.35 m/s

Westerschelde
averaged velocity

DELFT HYDRAULICS

Fig 2.6

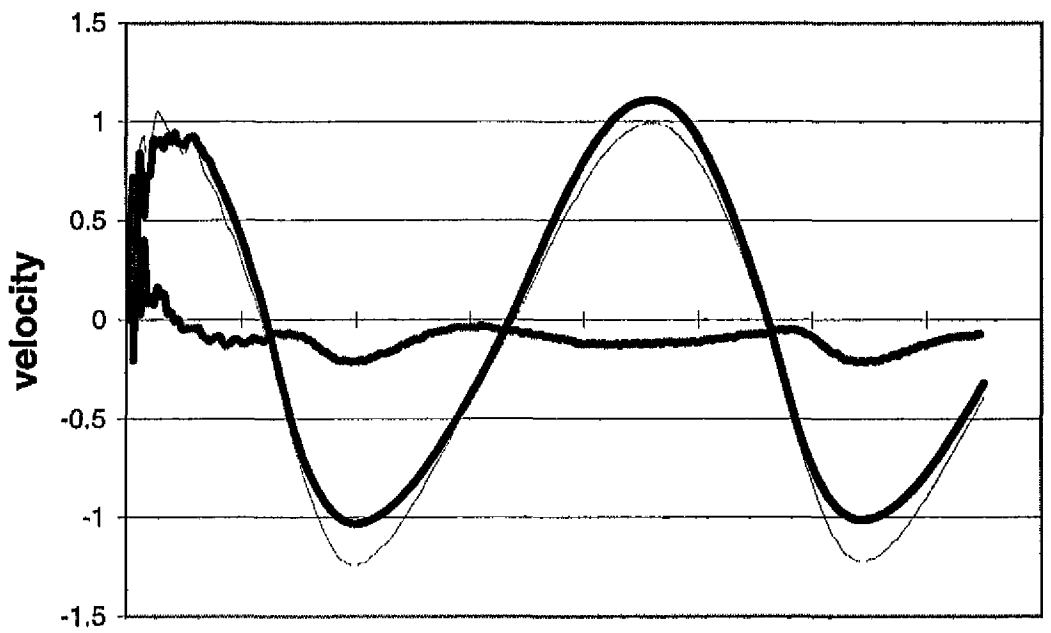

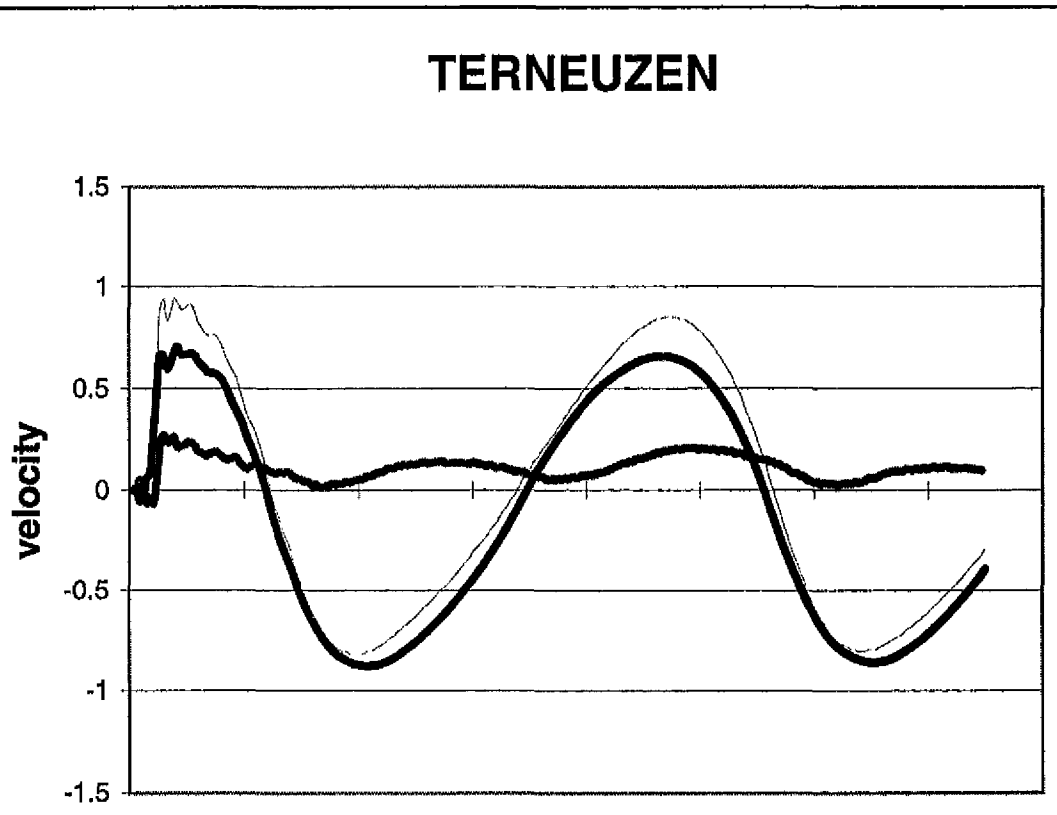

Velocity in IMPLIC and SOBEK in the final calibration of the water flow	Z919
DELFT HYDRAULICS	Figure 2.7

BATH

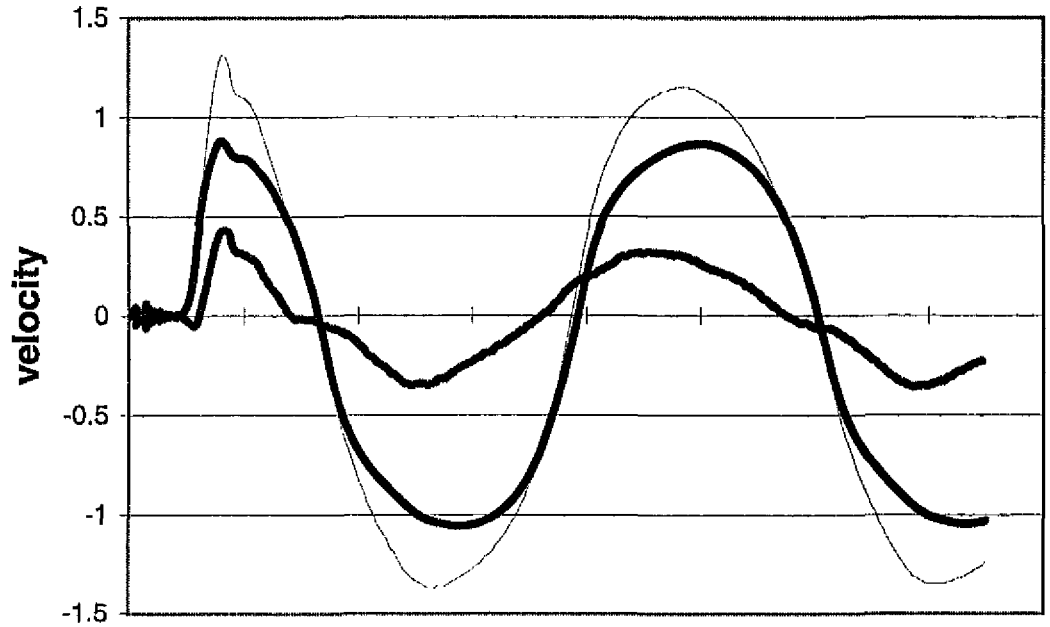

ANTWERPEN

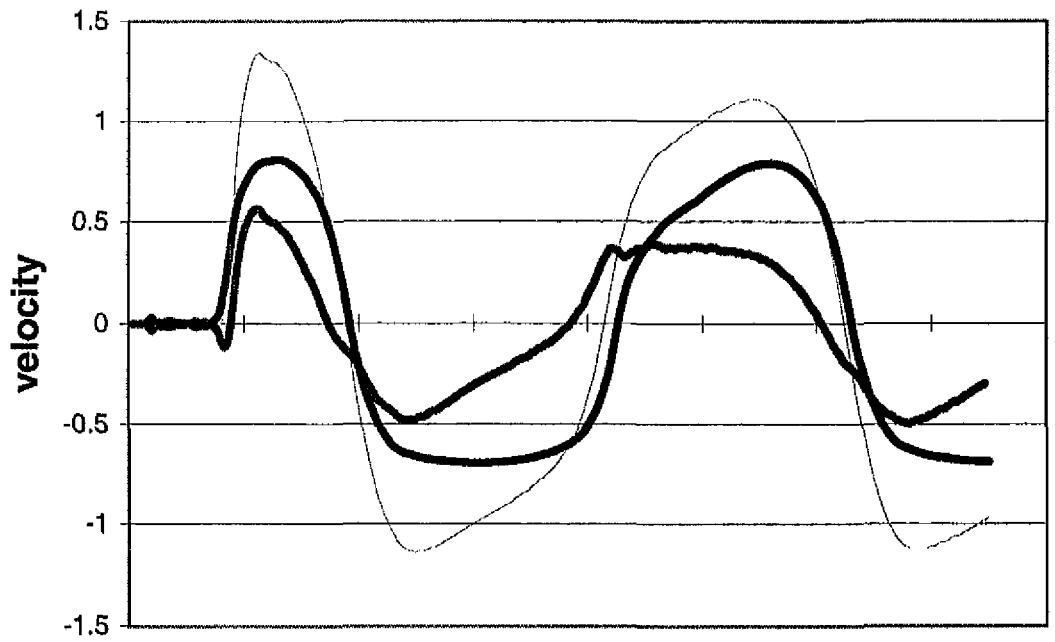

Velocity in IMPLIC and SOBEK in the final calibration of the water flow	Z919
DELFT HYDRAULICS	Figure 2.7

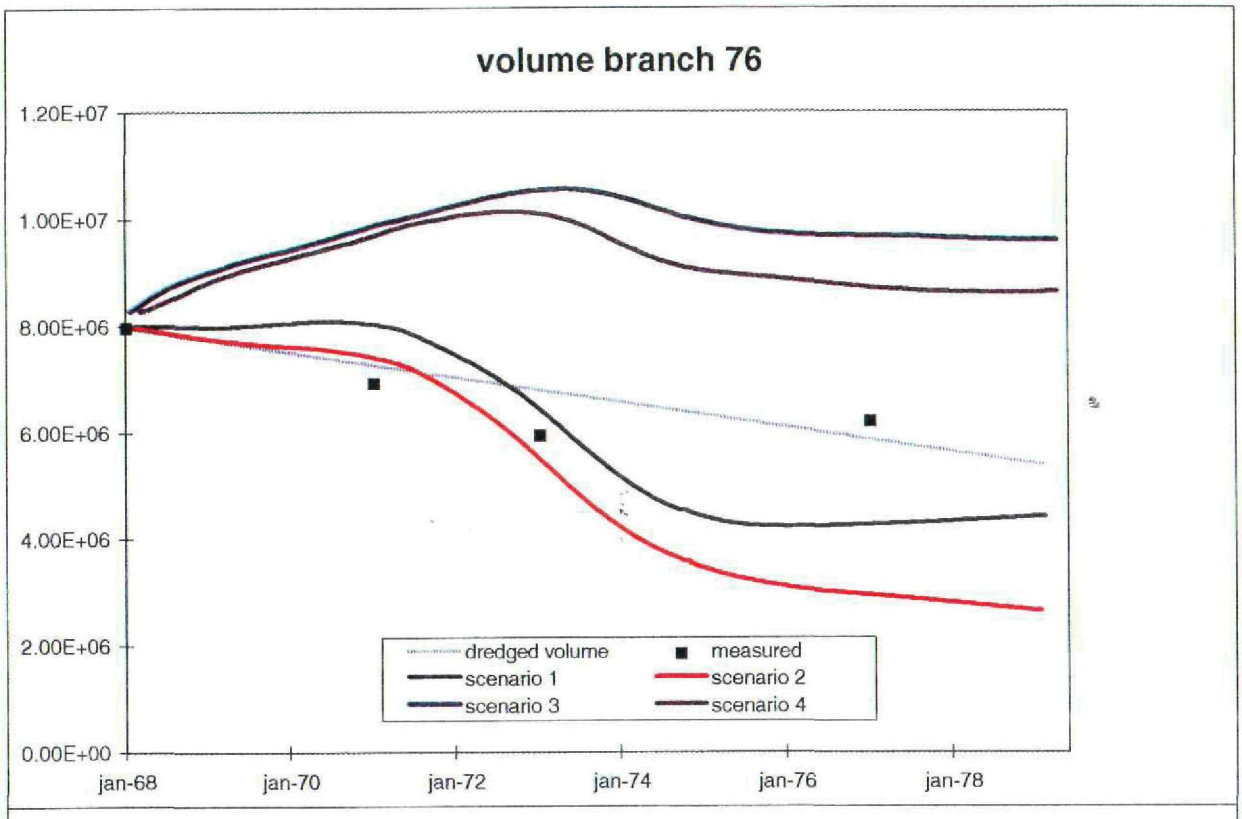

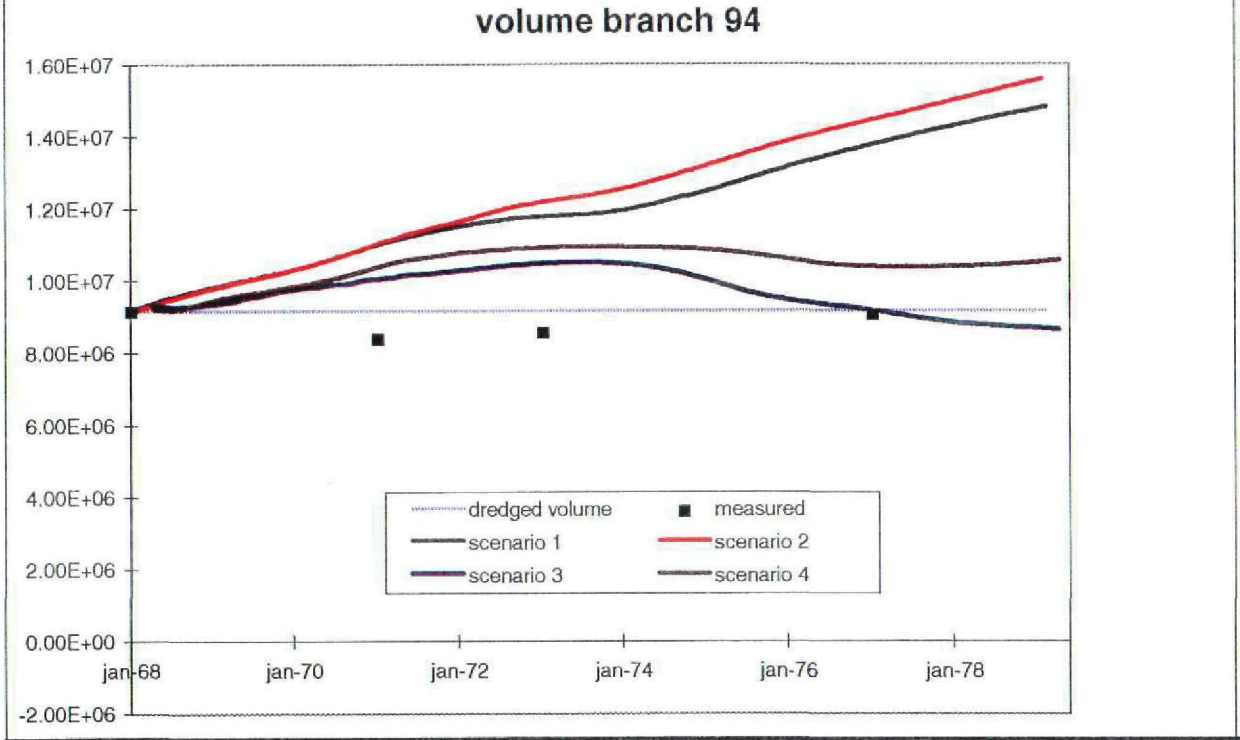

The development of the ebb channel and the flood channel Channel between Hansweert and Bath Ebb channel = branch 94; Flood channel = branch 76	Z919
DELFT HYDRAULICS	Figure 4.2

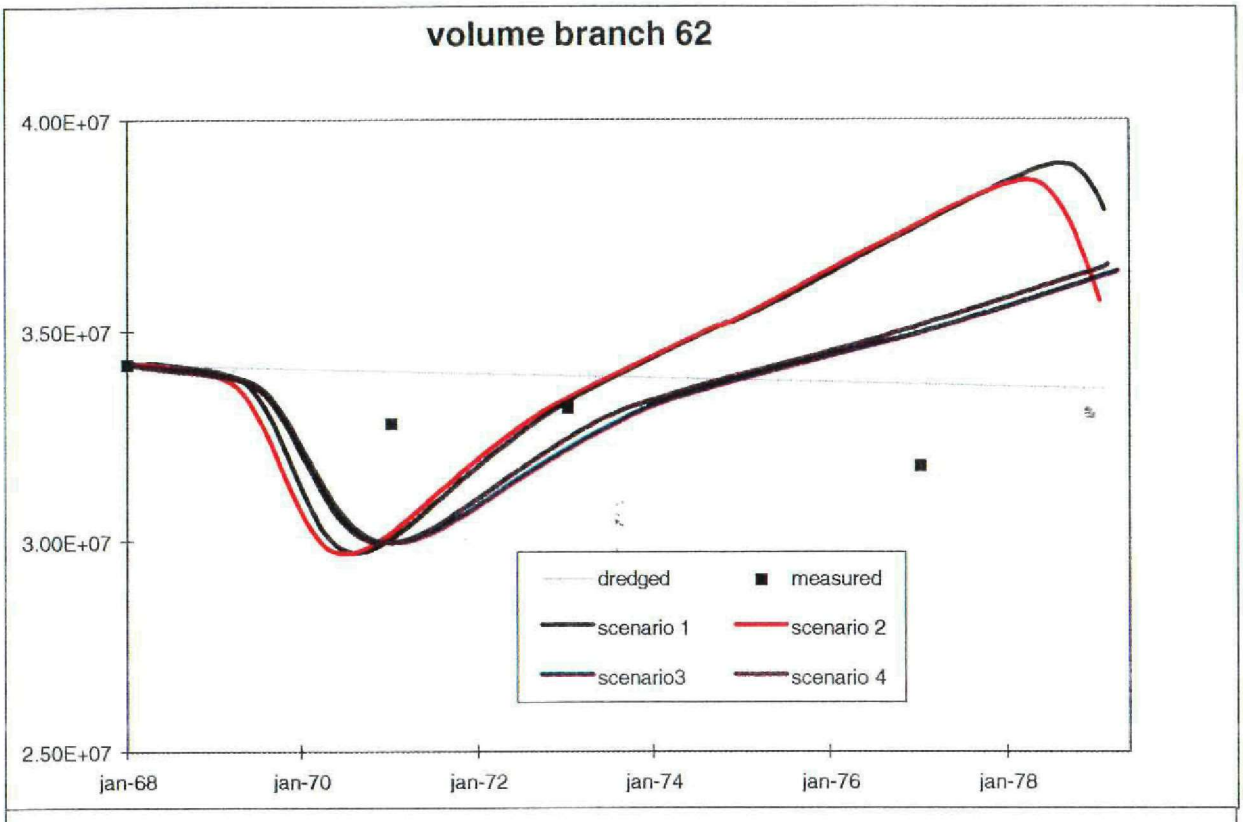

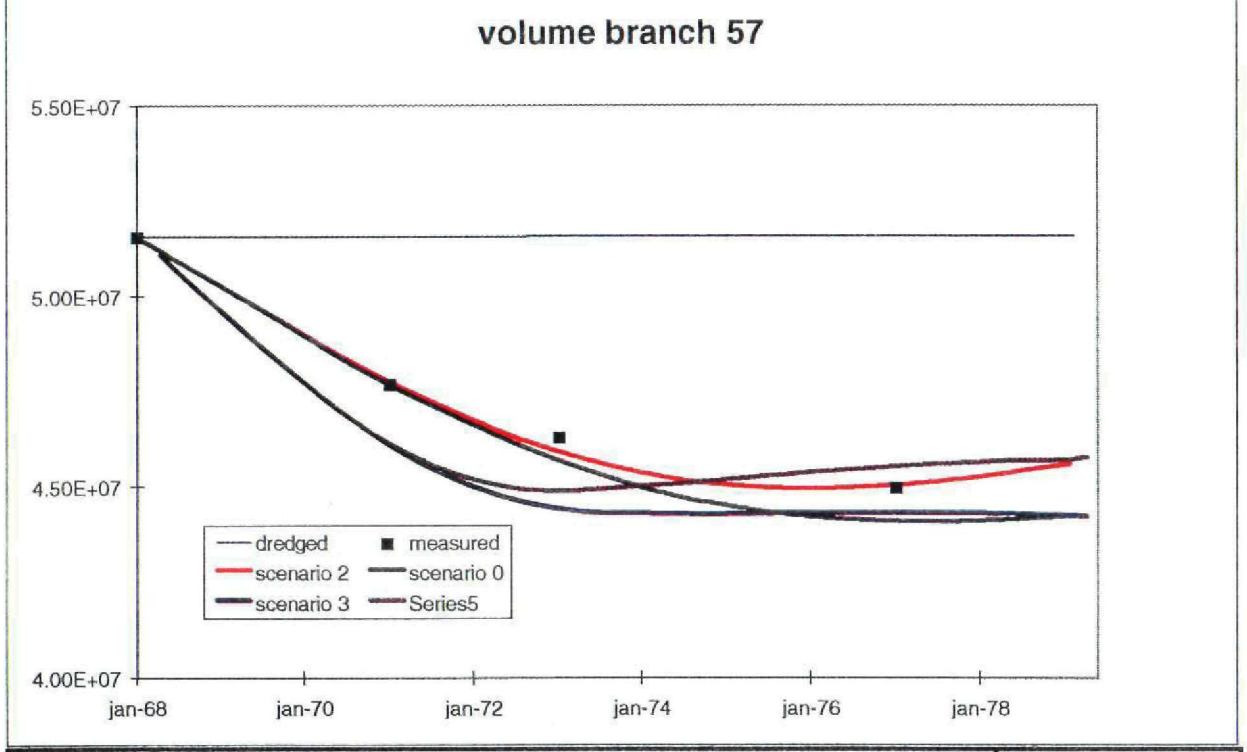

The development of the ebb channel and the flood channel Channel between Terneuzen and Hansweert Ebb channel = branch 62; Flood channel = branch 57	Z919
DELFT HYDRAULICS	Figure 4.2

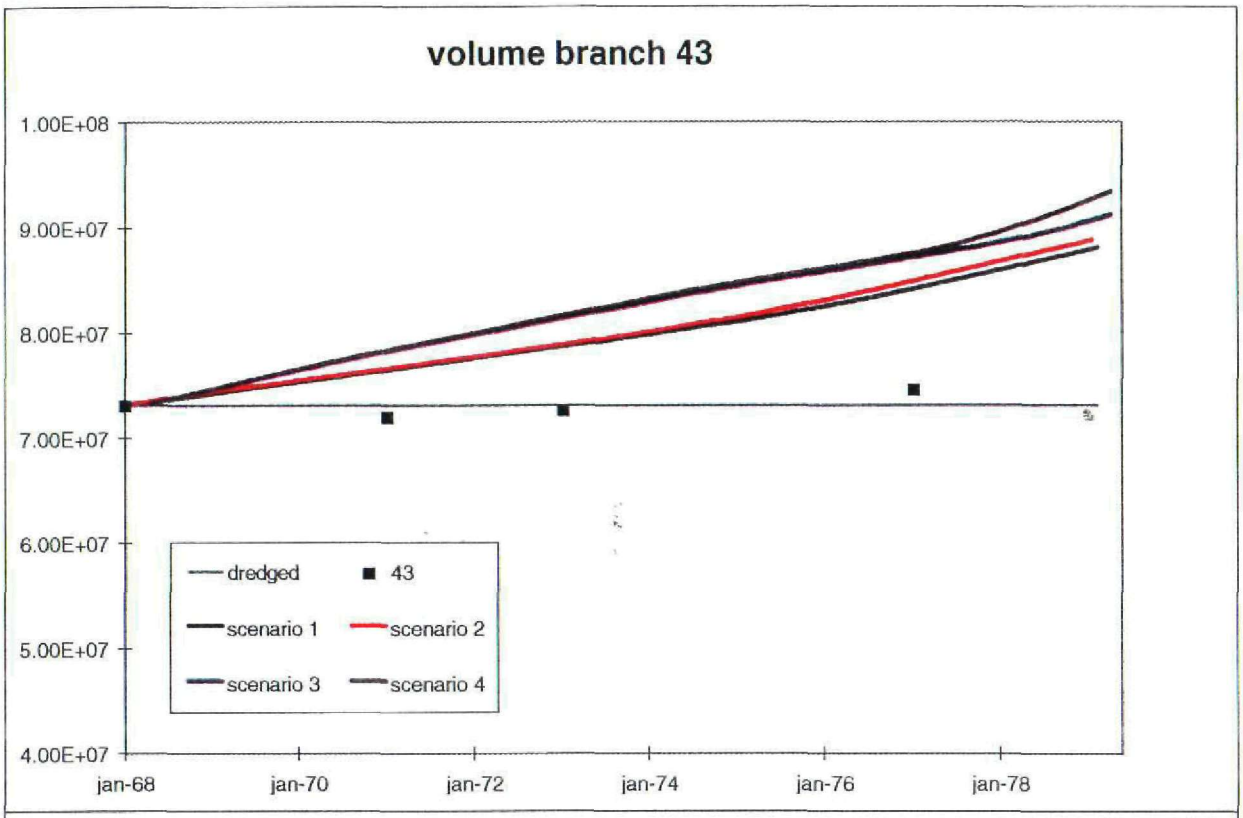

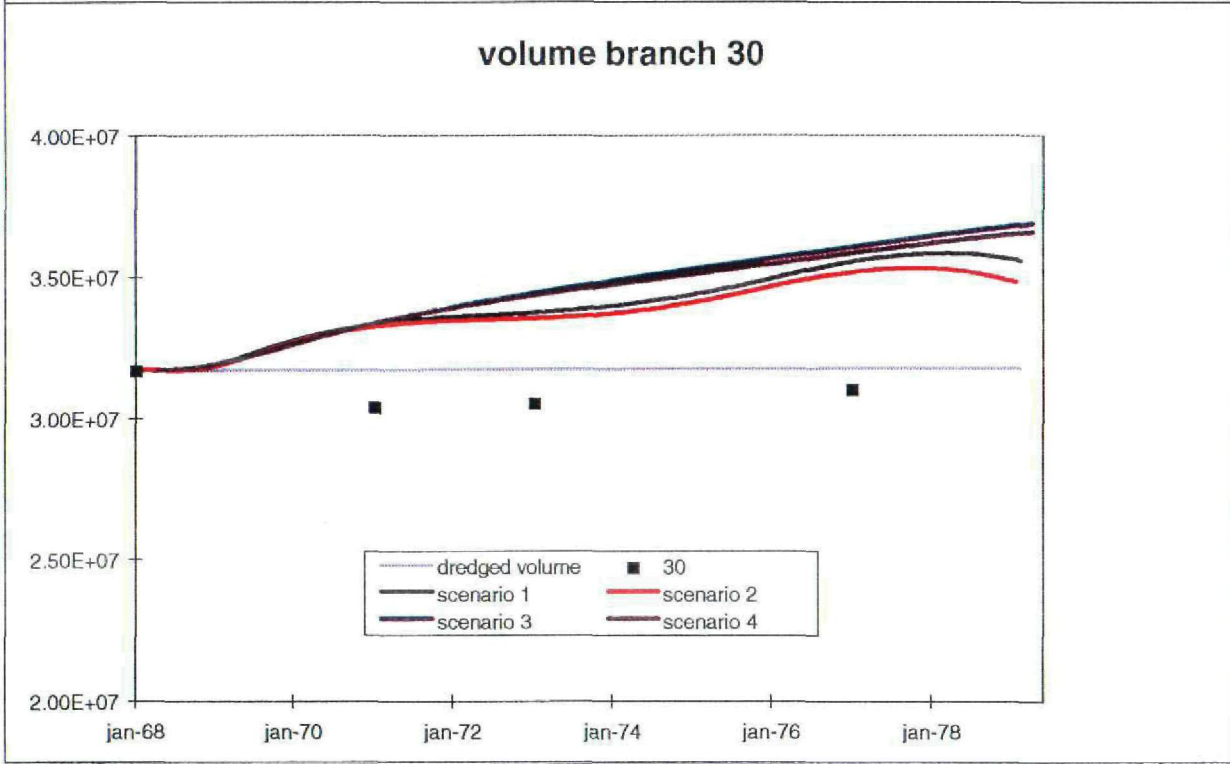

The development of the ebb channel and the flood channel Channel between Vlissingen and Terneuzen Ebb channel = branch 30; Flood channel = branch 43	Z919
DELFT HYDRAULICS	Figure 4.2